CONVEX MODELING BASED TOPOLOGY OPTIMIZATION WITH LOAD UNCERTAINTY

BY

XIKE ZHAO

A dissertation submitted to the

Graduate School-New Brunswick

Rutgers, The State University of New Jersey

In partial fulfillment of the requirements

For the degree of

Doctor of Philosophy

Graduate Program in Mechanical and Aerospace Engineering

Written under the direction of

Professor Hae Chang Gea

And approved by

_____

_____

_____

_____

New Brunswick, New Jersey

October, 2013

ABSTRACT OF THE DISSERTATION

CONVEX MODELING BASED TOPOLOGY OPTIMIZATION WITH LOAD UNCERTAINTY

by Xike Zhao

Dissertation Advisor:

Dr. Hae Chang Gea

In traditional topology optimization formulation the external load are deterministic and the uncertainties are not considered. The convex modeling based topology optimization method for solving topology optimization problems under external load uncertainties is presented in this dissertation. The load uncertainties are formulated using the non-probabilistic based unknown-but-bounded convex model. The sensitivities are derived and the problem is solved using gradient based algorithm. The proposed convex modeling based method yields the material distribution which would optimize the

worst structure response under the uncertain loads. Comparing to the deterministic based topology optimization formulation, the proposed method provided more reliable solutions when load uncertainties were involved. The proposed method can work with other method to solved complicated design problems. A protective structure design problem involving load uncertainties, multiple design objectives and unconstrained structure is solved by integrating the convex modeling based topology optimization method with regional strain energy formulation and inertial relief method. The simplicity, efficiency and versatility of the proposed convex modeling based method can be considered as a supplement to the sophisticated probabilistic based topology optimization methods.

Acknowledgements

This dissertation could never be finished without the help and support from lots of people. My deepest appreciation firstly goes to my advisor Professor Hae Chang Gea for his constant support and guidance throughout my doctoral studies. His passion for truth and rigorous attitude motivated me in both academic and personal aspects of my life.

I would also like to express my gratitude to my committee members, Professor Mitsunori Denda, Professor Liping Liu and Professor Kang Li for their valuable advises and encouragements.

My thankfulness goes to my lab mates: Dr. Euihark Lee, Dr. Kazuko Fuchi, Dr. Po Ting Lin, Dr. Xiaobao Liu, Dr. Zheqi Lin, Dr. Xiaoling Zhang, Dr. Yiru Ren, Wei Song, Huihui Qi, Bo Wang, Xiao Lin and Maneesh Raavi, for their help and support during the past five years. My thanks also goes to my colleges: Han Sun, Jiandong Meng, Jian Jiao, Lei Wang, Sunny Wong, Jianfeng Chen, Peinan Ge, Lixin Hu, Yang Wang, Hadi Halim and Gobong(Paul) Choi.

Most importantly I would like to thank my family: my father Wulin Zhao, my mother Jin Lu, my cousins Yuanjia Wang and Aolin Xie, and cousins-in-law Heedong Yun and Lidong Pan, I could never have accomplished this without you.

Lastly I would like to devote my gratefulness to my fiancée Wenhao Zhu for her love, accompany and sacrifice.

Dedications

To my parents

Wulin Zhao

Jin Lu

and my fiancé

Wenhao Zhu

13elieve

Table of Contents

List of Figures

List of Tables

Chapter 1
Introduction

For centuries engineers have been striving to design better structures like higher stiffness with less material usage [1]. Numerous methods have been proposed and in many of them design parameters (e.g. loads, structural geometries, and material properties) are assumed to be deterministic: in other words, possible uncertainties of the parameters are not considered in these methods. However, it is not always possible to avoid the uncertainties in engineering applications. Uncertainties could be brought into the structural design problem from various sources. Measurement errors, inaccuracy in the manufacturing process and perturbations in the external environment for example, are possible sources of uncertainties. Safety of the design given by the deterministic methods cannot be guaranteed when uncertainties are involved.

The uncertainties must be formulated into the structural design problem in order to reach a more reliable solution. Many approaches have been developed and generally they can be cataloged into probabilistic-based methods and non-probabilistic-based methods.

The probabilistic methods are established on the statistical analysis of the uncertain parameters. Under this uncertainty model the design problem can be formulated as optimizing the design target subject to prescribed reliability constraints (Reliability Based Design Optimization, RBDO) [2-4]. However it is worth noting that the probabilistic-based methods heavily rely on the accuracy of the statistical analysis. It is

shown that insufficient number of samples could induce large errors into the reliability calculation [5] and render the probabilistic based design result meaningless.

The non-probabilistic methods, including the convex model, the interval set and the fuzzy set, do not require the probability information. Therefore they can be utilized when such information is not available. Among them the convex model, which was proposed by Ben-Haim and Elishakoff in 1990 [6], represents the uncertainties by their extreme values and is ideal to treat the unknown-but-bounded uncertainties, which is one of the most common types of uncertainties in engineering application.

In these approaches the worst system response[1] under given uncertain stimulation is used as the benchmark for system performance evaluation. The possibilities of the system reaching the extremes need not to be calculated hence the probability information would not be required. Based on this framework, the design problem can be formulated as optimizing the design target subject to the constraint that the worst situation within the uncertainty bounds satisfies the design requirement (Worst Case Design Optimization, WCDO) [7]. As an alternative to the RBDO approaches, the WCDO has been investigated by a number of studies. Elishakoff et al proposed a convex model based non-probabilistic safety factor method [8]; Pantelides and Ganzerli also demonstrated a robust truss optimization approach [9] based on the convex models. The Eigenvalue Superposition of Convex Models (ESCM) formulation described in Chapter 2 [10] also

[1] Worst here means opposite to the desired value, for example largest stress when small stress is preferred

utilized the convex model and significantly increased the efficiency in solving truss design optimization problems under load uncertainties.

In this dissertation, a structural design optimization problem is formulated under the non-probabilistic WCDO framework as expressed below:

$$\begin{aligned} \min_{\boldsymbol{a}} \quad & w = w(\boldsymbol{a}) \\ \text{s.t.} \quad & \left[g_j(\boldsymbol{a}, \boldsymbol{f})\right]_{\max} \le 0 \\ & E(\boldsymbol{f}) \le 0 \end{aligned} \tag{1-1}$$

The objective function w can be any desired structure property and the constraint function $\max_{\boldsymbol{f}}[g_j(\boldsymbol{a}, \boldsymbol{f})] \le 0$ confines the worst system response. The $E(\boldsymbol{f}) \le 0$ constraint represents the bounds on the uncertainties of the stimulation $\boldsymbol{f}$ and the actual expression is problem dependent.

The expression in Eq.(1-1) can be expanded into a two-level optimization problem: the upper level problem focus on optimizing the structure and the lower level problem locates the worst case scenario. By defining $\left[g_j(\boldsymbol{a}, \boldsymbol{f})\right]_{\max} = g_{\max,j}$, the upper level problem, which gives the optimum design, can be expressed as:

$$\begin{aligned} \min_{\boldsymbol{a}} \quad & w = w(\boldsymbol{a}) \\ \text{s.t.} \quad & g_{\max,j}(\boldsymbol{a}) \le 0,\ j = 1 \ldots n \end{aligned} \tag{1-2}$$

And the lower level problem, that finds the worst structural response, is defined as:

$$\begin{aligned} \max_{\boldsymbol{f}} \quad & g_i(\boldsymbol{f}) \\ \text{s.t.} \quad & E(\boldsymbol{f}) \le 0 \end{aligned} \tag{1-3}$$

The design variable $\boldsymbol{a}$ is considered as constant in the lower level problem.

It is obvious that identifying the correct worst case scenario requires the lower level problem to be solved to its global optimality, otherwise the feasibility in the upper

level problem cannot be guaranteed. However as pointed out by Ben-Haim and Elishakoff in [6] and will be shown in the following chapters, in many situations the lower level problems might not always be convex, in fact in majority of the situations they are concave [6], and consequently their global optimality mighty be difficult to achieve. As mentioned above obtaining the global optima in the lower level problem is crucial for the WCDO framework, since the structure performance must be evaluated at its worst situation. In addition to the non-convex challenge the computational cost presents as another concern. If the lower level problems were solved by iterative methods then the iterations must be performed for every design step in the upper level problem. For instance if it would take 100 iterations to solve the lower level problem and there were 100 design steps in the upper level, a total number of 10000 iterations must be performed to reach the final design. For computational intense problems such as the topology optimization problems this approach is impractical. Finally in the two-level formulation the solution of the lower level problem served as constraints in the upper level design problem. The sensitivities of these constraints might not be able to be directly derived due to the absence of explicit expressions and the lack of sensitivity information would worsen the situation.

To overcome the obstacles, the convex modeling based topology optimization method was developed. This method was applied to a protective structure design problem with load uncertainties and the sensitivity was analyzed.

1.1 Research Contribution

The structure design under external load uncertainty problem was investigated in this dissertation. The uncertainties are formulated using convex model based unknown-but-bounded uncertainty model. The Eigenvalue Superposition of Convex Models method was developed for solving truss size optimization problems. The ESCM concept was then extended to topology optimization yielding the convex modeling based topology optimization method for solving structure design problems with external load uncertainties. The sensitivity was analyzed and numerical examples were shown. Finally the convex modeling based method was utilized in solving the protective structure design problem together with other methods.

1.2 Out Line of the Dissertation

In this dissertation the for convex modeling based method solving structure design problem under external load uncertainties was proposed. The research background and motivation was introduced in Chapter 1. In Chapter 2 the ESCM method for solving truss size optimization problem was derived. The derivation started from solving a single uncertainty problem by constructing an eigenvalue problem; the multiple-uncertainty problem was then solved through superposition of the solutions of single uncertainty sub problems. The effectiveness of the ESCM method was demonstrated through numerical

examples. The proposed method is extended to topology optimization in Chapter 3. Sensitivity analysis was performed and the result obtained from the new convex modeling based topology optimization was compared with results from traditional methods. In Chapter 4 a protective structure design problem involving external load uncertainty, multiple-objective optimization and unconstrained structure was analyzed by integrating the convex modeling based topology optimization method with regional strain energy formulation and inertial relief method. Conclusions were made in Chapter 5 as well as possibilities for future research.

Chapter 2

ESCM Method in Truss Design Optimization

Being characterized as *"... a structure composed of slender members joined together at their end points"* by Hibbeler [11], trusses have been widely applied in various of fields for centuries and have been intensively studied by numerous engineers, scientists and mathematicians from many different aspects. Early studies of trusses could be traced back to the age of ancient Rome more than two thousand years ago [1]. Throughout the years engineers are searching for designs which would best meet the demand and the methods for optimizing truss structures are sophisticated.

2.1 Introduction to Truss Design Optimization

The modern design optimizations of truss structures generally fall into three categories [12]: 1). The Size Optimization; 2). The Geometry Optimization; and 3). The Topology Optimization.

In the size optimization problem, the geometries and the topologies of the truss structures are considered as fixed. The sizes of the truss elements, cross section areas for example, are the design variables and the design objective is optimized [13].

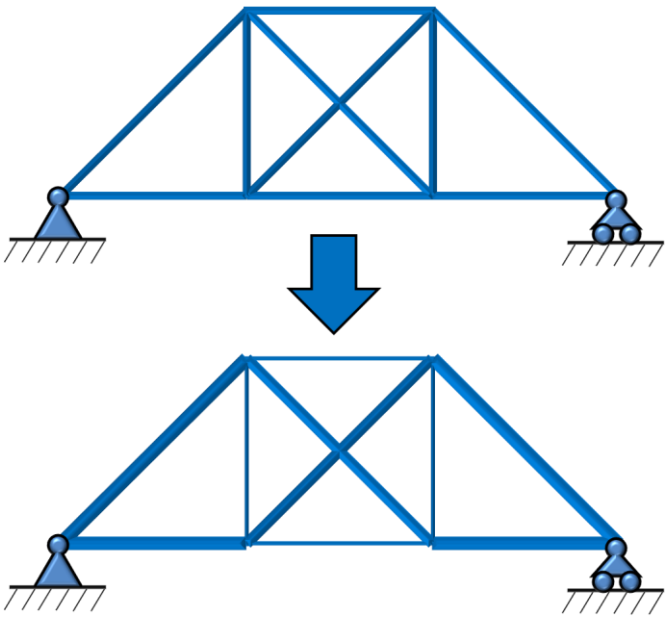

Figure 2-1. The Size Optimization

For the geometry optimization, the design variables are the coordinates of the joints of the truss elements.

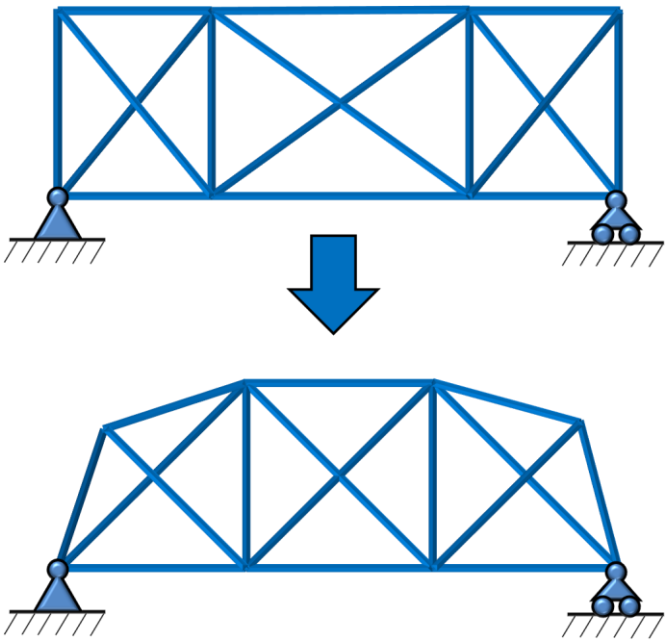

Figure 2-2. The Geometry Optimization

In the topology optimization, the connectivity of truss elements is the design variable and the layout of the structure is optimized.

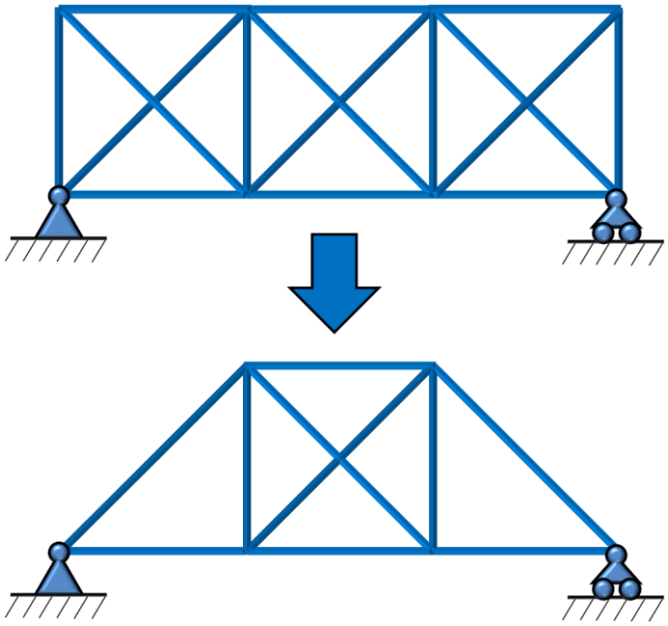

Figure 2-3. The Topology Optimization

Among the three, the size optimization is the focus of this dissertation due to its broad range of applications [14]. It is the fundamental problem in truss design optimization and its versatility can be seen from the fact that by properly setting the initial design and design variable lower bound, the size optimization approach can be used to solve topology optimization problems.

2.2 Truss Design Optimization

To better illustrate the problem, a simple truss structure design optimization problem is considered here, as shown in Figure 2-4.

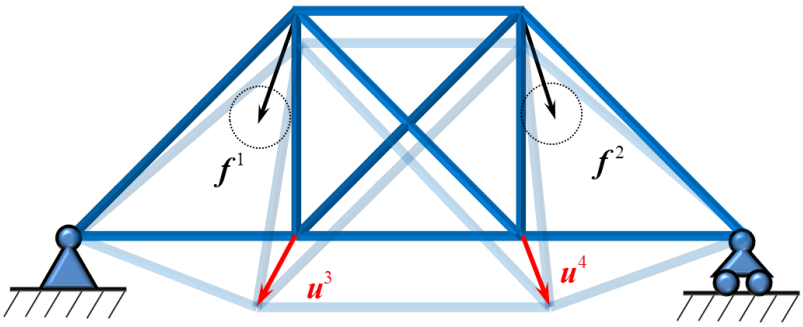

Figure 2-4. Structure under External Load Uncertainties

Two external loads with uncertainties in both directions and magnitudes, $\boldsymbol{f}^1$ and $\boldsymbol{f}^2$, are applied to the structure at Node 1 and Node 2. The design objective is to find the optimum cross section areas of the bars which minimize the total weight of the structure. The design requirement is that the maximum magnitudes of displacements of Node 3 and Node 4 must not exceed given values. The structure can be discretized by finite element method as $\boldsymbol{K}\boldsymbol{u} = \boldsymbol{f}$ and the nodal displacement vector of j^{th} node $\boldsymbol{u}^j$ can be expressed as

$$\boldsymbol{u}^j = \boldsymbol{B}_j \boldsymbol{u} = \boldsymbol{B}_j^T \boldsymbol{K}^{-1} \boldsymbol{f}$$

where $\boldsymbol{K}$ is the global stiffness matrix, $\boldsymbol{B}_j$ is a localization matrix and the index j indicates the j^{th} node. The global load vector $\boldsymbol{f}$ can alternatively be expressed as the assembly of the nodal load vector $\boldsymbol{f}^i$,as

$$\begin{aligned} \boldsymbol{A}_i^T \boldsymbol{f} &= \boldsymbol{f}^i \\ \boldsymbol{f} &= \sum_i^n \boldsymbol{A}_i \boldsymbol{f}^i \end{aligned} \qquad (2\text{-}1)$$

where $\boldsymbol{A}_i$ is another localization matrix, and the summation should be understood as assembly. The matrices $\boldsymbol{B}_j$ and $\boldsymbol{A}_i$ have the form of

$$\begin{bmatrix} 0 & \cdots & 1 & 0 & \cdots & 0 \\ 0 & \cdots & 0 & 1 & \cdots & 0 \end{bmatrix}^T$$

and they give the relation between the 2×1 nodal vectors and the $m\times1$ global vector, where m is the total DOFs.

2.2.1 Unknown-but-Bounded Uncertainty Formulation

The uncertainties in the external loads are formulated with the unknown-but-bounded model, which is a typical convex model. The name of the model explains itself: although the exact value the parameter is unknown, the variation is within a known range. In this model the variable x with uncertainty is decomposed into its nominal value $\bar{x}$ and deviation Δx. The nominal value is considered deterministic and the deviation is bounded. The exact formulation of this model is problem dependent and for the external loads in the Figure 2-4 problem, which are assumed to have uncertainties in both magnitudes and directions, the uncertainty formulation is introduced as follow.

The nodal load vector $\boldsymbol{f}^1$ decomposed into its nominal value and deviation $\boldsymbol{f}^1 = \overline{\boldsymbol{f}^1} + \Delta\boldsymbol{f}^1$. The nominal term $\overline{\boldsymbol{f}^1}$ is constant and the magnitude of the deviation $\Delta\boldsymbol{f}^1$ is confined to be smaller or equal to a given value c_1, as expressed in Eq.(2-2).

$$\begin{aligned} \boldsymbol{f}^1 &= \overline{\boldsymbol{f}^1} + \Delta\boldsymbol{f}^1 \\ \left\|\Delta\boldsymbol{f}^1\right\|^2 &= \left(\Delta\boldsymbol{f}^1\right)^T \Delta\boldsymbol{f}^1 \le c_1 \end{aligned} \tag{2-2}$$

This expression can be visualized in Figure 2-5, where the load $\boldsymbol{f}^1$ perturbs within the shaded circular area defined by $\overline{\boldsymbol{f}^1}$ and $\left\|\Delta\boldsymbol{f}^1\right\|$.

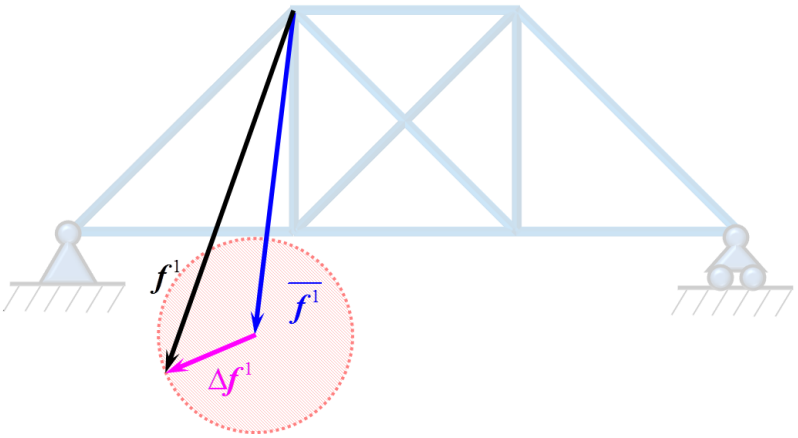

Figure 2-5. The Unknown-but-Bounded Uncertainty Formulation

It should be noted that without losing generosity, the bound value c_1 in Eq.(2-2) can be normalized and yields the following simplified uncertainty formulation

$$\begin{aligned} \boldsymbol{f}^i &= \overline{\boldsymbol{f}^i} + \Delta\boldsymbol{f}^i \\ \left\|\Delta\boldsymbol{f}^i\right\|^2 &\le 1 \end{aligned} \tag{2-3}$$

which can also be expressed by using the global load vector $\boldsymbol{f}$ as

$$\begin{aligned} \boldsymbol{f} &= \overline{\boldsymbol{f}} + \Delta\boldsymbol{f} \\ \Delta\boldsymbol{f}^T \boldsymbol{A}_i \boldsymbol{A}_i^T \Delta\boldsymbol{f} &\le 1 \end{aligned} \tag{2-4}$$

The above unknown-but-bounded uncertainty model defined in Eq.(2-3) and Eq.(2-4) is used in the derivation of this research.

2.2.2 Problem Formulation

Implementing the uncertainty model shown in Eq.(2-3) into Eq.(1-1) gives the complete explicit expression for the structural design optimization problem defined in Figure 2-4, as described below

$$\begin{aligned} \min_{\boldsymbol{a}} \quad & w = w(\boldsymbol{a}) \\ \text{s.t.} \quad & \left\| \boldsymbol{u}^j(\boldsymbol{a}) \right\|_{\max} \le d_j \\ & \boldsymbol{f}^i = \overline{\boldsymbol{f}^i} + \Delta \boldsymbol{f}^i \\ & \left\| \Delta \boldsymbol{f}^i \right\|^2 \le 1 \end{aligned} \tag{2-5}$$

This single level formulation can be extended into a two-level formulation in the same manner as Eq.(1-2) and Eq.(1-3). The upper level problem is straightforwardly expressed as

$$\begin{aligned} \min_{\boldsymbol{a}} \quad & w = w(\boldsymbol{a}) \\ \text{s.t.} \quad & \left\| \boldsymbol{u}^j(\boldsymbol{a}) \right\|_{\max} \le d_j \end{aligned} \tag{2-6}$$

For the lower level problem a trick is played to avoid the square root introduced by the vector norm. Instead of using the original objective function $\left\| \boldsymbol{u}^j \right\|$, the squared term

$$\left\| \boldsymbol{u}^j \right\|^2 = \left(\sqrt{\left(\boldsymbol{u}^j \right)^T \boldsymbol{u}^j} \right)^2 = \left(\boldsymbol{u}^j \right)^T \boldsymbol{u}$$

is used. Thus the lower level formulation becomes

$$\begin{aligned} \max_{\boldsymbol{f}} \quad & \left\| \boldsymbol{u}^j \right\|^2 \\ \text{s.t.} \quad & \boldsymbol{f}^i = \overline{\boldsymbol{f}^i} + \Delta \boldsymbol{f}^i \\ & \left\| \Delta \boldsymbol{f}^i \right\|^2 \le 1 \end{aligned} \tag{2-7}$$

Expanding the norm terms and Eq.(2-7) is rewritten into

$$\begin{aligned} \max_{\boldsymbol{f}} \quad & \sum_i^n \left[\left(\boldsymbol{f}^i \right)^T \boldsymbol{A}_i^T \boldsymbol{K}^{-T} \boldsymbol{B}_j \boldsymbol{B}_j^T \boldsymbol{K}^{-1} \boldsymbol{A}_i \boldsymbol{f}^i \right] \\ \text{s.t.} \quad & \boldsymbol{f}^i = \overline{\boldsymbol{f}^i} + \Delta \boldsymbol{f}^i \\ & \left(\Delta \boldsymbol{f}^i \right)^T \Delta \boldsymbol{f}^i \le 1 \end{aligned} \tag{2-8}$$

This formulation in Eq.(2-8) can alternatively be expressed using the global load vector $\boldsymbol{f}$ instead of the nodal vectors $\boldsymbol{f}^i$, which yields

$$\begin{aligned} \max_{\boldsymbol{f}} \quad & \boldsymbol{f}^T \boldsymbol{K}^{-T} \boldsymbol{B}_j \boldsymbol{B}_j^T \boldsymbol{K}^{-1} \boldsymbol{f} \\ \text{s.t.} \quad & \boldsymbol{f} = \overline{\boldsymbol{f}} + \Delta \boldsymbol{f} \\ & \Delta \boldsymbol{f}^T \boldsymbol{A}_i \boldsymbol{A}_i^T \Delta \boldsymbol{f} \le 1 \end{aligned} \tag{2-9}$$

Quadratic forms are observed in both the objective function and the constraint functions in Eq.(2-9). The problem in Eq.(2-9) is a typical Quadratically Constrained Quadratic Programming (QCQP) problem. Since the matrices $\boldsymbol{K}$ and $\boldsymbol{B}_j$ are positive semi-definite (P.S.D), as proven in [15], the resultant matrix $\boldsymbol{Q} = \boldsymbol{K}^{-T} \boldsymbol{B}_j \boldsymbol{B}_j^T \boldsymbol{K}^{-1}$ is either a zero matrix or a P.S.D matrix with zero matrix leads to a trivial solution. This problem is a well-known non-convex minimization problem and is classified as NP-Hard problem [16-18].

The non-convexity of this lower level problem can be visualized through a simple example. Consider the structure under one load with uncertainty shown in Figure 2-6

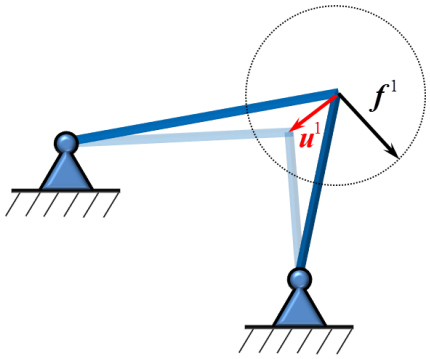

Figure 2-6. The 3-Node 2-Element Structure

The load $\boldsymbol{f}^1$ has known maximum magnitude and uncertain direction. The magnitude of displacement $\|\boldsymbol{u}^1\|$ is concerned. The mathematical formulation is established as

$$\begin{aligned} \min_{\boldsymbol{f}} \quad & -\left\|\boldsymbol{u}^1\right\|^2 \\ \text{s.t.} \quad & \left\|\boldsymbol{f}^1\right\|^2 \le c \end{aligned} \tag{2-10}$$

Noted that by convention the objective is changed from a maximized positive to a minimized negative. The design domain of the Eq.(2-10) can be plotted as

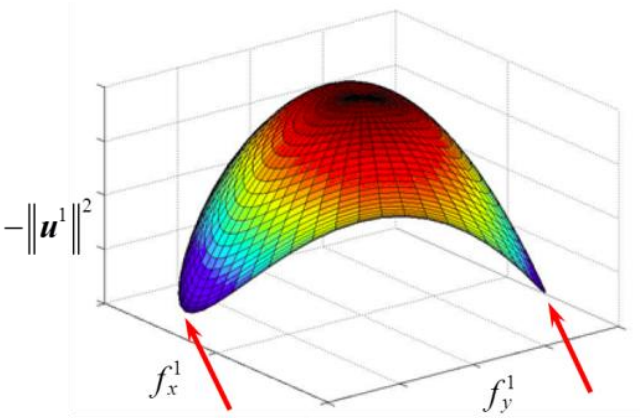

Figure 2-7. Feasible Domain of Eq.(2-10) Problem

The colored contour represents the objective function. The domain is clearly concave and multiple local optima can be identified in Figure 2-7. As mentioned before, this non-convexity would make solving the problem through conventional gradient based method impractical.

The non-convexity problem of the WCDO has been studied in the literature. Elishakoff et al proposed a convex model based on the non-probabilistic safety factor method [8]. Pantelides and Ganzerli demonstrated a robust truss optimization method [9]. Approaches utilizing interval linear algebra for Uncertain Linear Equations (ULE) [19] is also proposed [20]. Semi-Definite Programming (SDP) [21] relaxation method is introduced to find the response ellipsoidal bounds [22, 23]. Particularly for the problems involving uncertainties on the external loads, which is the focus of this research, the

Quadratically Constraint Quadratic Programming (QCQP) formulations is often used, and they can be solved through the SDP relaxation method, as given in [24].

2.2.3 SDP Relaxation Method

The SPD relaxation method conservatively approximates the global optima of the Eq.(2-7) lower level problem by relaxing it into the SDP problem. As remarked by Vandenberghe [25], the resultant SDP problems are convex optimization problems and their global optimum can be obtained by many well-established algorithms [26].

To be specific, the Lagrangian of the Eq(2-9) lower level problem

$$\begin{aligned} \max_{\boldsymbol{f}} \quad & \boldsymbol{f}^T \boldsymbol{K}^{-T} \boldsymbol{B}_j \boldsymbol{B}_j^T \boldsymbol{K}^{-1} \boldsymbol{f} \\ \text{s.t.} \quad & \boldsymbol{f} = \overline{\boldsymbol{f}} + \Delta \boldsymbol{f} \\ & \Delta \boldsymbol{f}^T \boldsymbol{A}_i \boldsymbol{A}_i^T \Delta \boldsymbol{f} \le 1 \end{aligned}$$

can be written as

$$\begin{aligned} L &= -\boldsymbol{f}^T \boldsymbol{K}^{-T} \boldsymbol{B}_j \boldsymbol{B}_j^T \boldsymbol{K}^{-1} \boldsymbol{f} + \textstyle\sum_i \lambda_i (\Delta \boldsymbol{f}^T \boldsymbol{A}_i \boldsymbol{A}_i^T \Delta \boldsymbol{f} - 1) \\ &= -\boldsymbol{f}^T \boldsymbol{Q} \boldsymbol{f} + \textstyle\sum_i \lambda_i (\Delta \boldsymbol{f}^T \boldsymbol{A}_i \boldsymbol{A}_i^T \Delta \boldsymbol{f} - 1) \\ &= -(\overline{\boldsymbol{f}} + \Delta \boldsymbol{f})^T \boldsymbol{Q} (\overline{\boldsymbol{f}} + \Delta \boldsymbol{f}) + \textstyle\sum_i \lambda_i (\Delta \boldsymbol{f}^T \boldsymbol{A}_i \boldsymbol{A}_i^T \Delta \boldsymbol{f} - 1) \end{aligned} \tag{2-11}$$

The idea of relaxation is that instead of directly minimizing the Lagrangian, a lower bound is defined as

$$t \le L(\Delta \boldsymbol{f}, \lambda) \quad \forall \Delta \boldsymbol{f}$$

The bound is then tightened by an optimization problem

$$\begin{aligned} \max_{\Delta \boldsymbol{f}} \quad & t \\ \text{s.t.} \quad & L(\Delta \boldsymbol{f}, \lambda) - t \ge 0 \\ & t \ge 0 \end{aligned} \tag{2-12}$$

Performing homogenization on $L(\Delta \boldsymbol{f}, \lambda) - t \ge 0$ gives

$$\begin{pmatrix} \Delta \boldsymbol{f} \\ 1 \end{pmatrix}^T \begin{pmatrix} -\boldsymbol{Q} + \sum_i \lambda_i \boldsymbol{A}_i \boldsymbol{A}_i^T & -\boldsymbol{Q}\bar{\boldsymbol{f}} \\ -(\boldsymbol{Q}\bar{\boldsymbol{f}})^T & -\bar{\boldsymbol{f}}^T \boldsymbol{Q}\bar{\boldsymbol{f}} - \sum_i \lambda_i - t \end{pmatrix} \begin{pmatrix} \Delta \boldsymbol{f} \\ 1 \end{pmatrix} \geq 0$$

which is equivalent to

$$\begin{pmatrix} -\boldsymbol{Q} + \sum_i \lambda_i \boldsymbol{A}_i \boldsymbol{A}_i^T & -\boldsymbol{Q}\bar{\boldsymbol{f}} \\ -(\boldsymbol{Q}\bar{\boldsymbol{f}})^T & -\bar{\boldsymbol{f}}^T \boldsymbol{Q}\bar{\boldsymbol{f}} - \sum_i \lambda_i - t \end{pmatrix} \geq 0 \tag{2-13}$$

The problem in Eq.(2-12) can therefore be reformulated as

$$\begin{aligned} \max_{\lambda_i} \quad & t \\ \text{s.t.} \quad & \begin{pmatrix} -\boldsymbol{Q} + \sum_i \lambda_i \boldsymbol{A}_i \boldsymbol{A}_i^T & -\boldsymbol{Q}\bar{\boldsymbol{f}} \\ -(\boldsymbol{Q}\bar{\boldsymbol{f}})^T & -\bar{\boldsymbol{f}}^T \boldsymbol{Q}\bar{\boldsymbol{f}} - \sum_i \lambda_i - t \end{pmatrix} \geq 0 \\ & t \geq 0 \end{aligned} \tag{2-14}$$

Note that the design variables have changed from $\Delta \boldsymbol{f}$ in Eq.(2-12) to λ_i in Eq.(2-14). The Eq.(2-14) is a standard SDP problem which can be solved by many well-established algorithms. The solution is given as

$$\left\| \boldsymbol{u}_{\max}^j \right\|^2 = \boldsymbol{f}^T \boldsymbol{Q} \boldsymbol{f} \leq t_{\max}$$

With this SDP solution, the upper level design problem in Eq.(2-6) can be written as

$$\begin{aligned} \min_{\boldsymbol{a}} \quad & w = w(\boldsymbol{a}) \\ \text{s.t.} \quad & \sqrt{t_{\max}(\boldsymbol{a})} \leq d_j \end{aligned}$$

Using the SPD relaxation technique, the concave lower level problem is relaxed into a convex SDP problem and the true solution of the original concave problem is conservatively approximated with solution of the convex SDP problem. However in this approach an optimization problem is still required to find the worst case scenario, which hampers the overall efficiency in solving the structure design problem.

2.3 Eigenvalue-Superposition of Convex Models (ESCM) Method

The eigenvalue-superposition of convex models (ESCM) approach is presented in this section to address the aforementioned challenges in solving the lower level problem. The derivation of the method starts from a single uncertainty truss structure design optimization problem. The multiple-uncertainties situation is then considered, followed by the sensitivity analysis.

2.3.1 Single Uncertainty Problem

Consider the structure with one uncertain load $\boldsymbol{f}^1 = \overline{\boldsymbol{f}^1} + \Delta\boldsymbol{f}^1$ applied, as shown in Figure 2-8. The problem is further simplified by neglecting the nominal load $\overline{\boldsymbol{f}^1}$ and assuming $\boldsymbol{f}^1 = \Delta\boldsymbol{f}^1$.

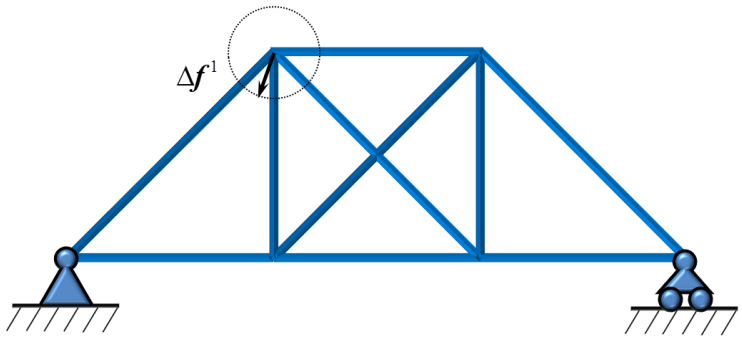

Figure 2-8. The Truss Structure under Single Uncertain Load

Following these assumptions, the lower level optimization problem can be described as

$$\begin{aligned} \max_{\Delta\boldsymbol{f}^1} \quad & \left\| \boldsymbol{u}^{j,\Delta f^1}(\Delta\boldsymbol{f}^1) \right\|^2 = \left(\Delta\boldsymbol{f}^1\right)^T \boldsymbol{Q}\Delta\boldsymbol{f}^1 \\ \text{s.t.} \quad & \left\|\Delta\boldsymbol{f}^1\right\|^2 = \left(\Delta\boldsymbol{f}^1\right)^T \Delta\boldsymbol{f}^1 \le 1 \end{aligned} \tag{2-15}$$

where $\boldsymbol{Q} = \boldsymbol{A}_i^T \boldsymbol{K}^{-T} \boldsymbol{B}_j \boldsymbol{B}_j^T \boldsymbol{K}^{-1} \boldsymbol{A}_i$. In fact this problem is essentially identical to the problem illustrated in Figure 2-6, which is concave and cannot be solved by conventional gradient search.

To tackle this problem, the Lagrangian of Eq.(2-15) is firstly examined, which is given as

$$L\left(\Delta \boldsymbol{f}^1, \lambda\right) = -\left(\Delta \boldsymbol{f}^1\right)^T \boldsymbol{Q} \Delta \boldsymbol{f}^1 + \lambda\left[\left(\Delta \boldsymbol{f}^1\right)^T \Delta \boldsymbol{f}^1 - 1\right] \tag{2-16}$$

The 1st order KKT conditions can then be established as

$$-\boldsymbol{Q}\Delta \boldsymbol{f}^{1*} + \lambda^* \Delta \boldsymbol{f}^{1*} = 0 \tag{2-17}$$

$$\left(\Delta \boldsymbol{f}^{1*}\right)^T \Delta \boldsymbol{f}^{1*} - 1 \le 0 \tag{2-18}$$

$$\lambda^* \ge 0 \tag{2-19}$$

$$\lambda^*\left[\left(\Delta \boldsymbol{f}^{1*}\right)^T \Delta \boldsymbol{f}^{1*} - 1\right] = 0 \tag{2-20}$$

The stationarity condition in Eq.(2-17) is indeed an eigenvalue problem with all eigenvalues of $\boldsymbol{Q}$ satisfies the equation. The primal feasibility condition in Eq.(2-18) on the other hand can be considered as the eigenvector normalization condition. The dual feasibility condition in Eq.(2-19) would be automatically satisfied since as mentioned before, the $\boldsymbol{Q}$ matrix is either a zero or P.S.D matrix, hence λ^*,which is the eigenvalue of $\boldsymbol{Q}$, must be non-negative. Finally the complementary slackness condition requires the constraint to be active in case $\boldsymbol{Q}$ being positive definite (P.D), due to the fact that λ^* must be positive in such condition.

By solving the 1st order KKT conditions, it can be identified that the optimum candidates are the eigenvalues of $\boldsymbol{Q}$. In order to determine the true optimum, the second order sufficient condition is then examined This 2nd order condition can be found as

$$-\boldsymbol{Q}+\lambda^{*}\boldsymbol{I}\succeq 0 \tag{2-21}$$

Performing eigen-decomposition on $\boldsymbol{Q}$ yields $\boldsymbol{Q}=\boldsymbol{V}\boldsymbol{D}\boldsymbol{V}^{T}$ where $\boldsymbol{D}$ is a diagonal matrix with eigenvalues of $\boldsymbol{Q}$ in the diagonal. The $\boldsymbol{V}$ is the matrix of eigenvectors. Since $\boldsymbol{Q}$ is P.S.D, $\boldsymbol{V}$ can be normalized as a unitary matrix, which implies $\boldsymbol{V}^{T}\boldsymbol{V}=\boldsymbol{I}$, $\boldsymbol{V}^{T}\boldsymbol{Q}\boldsymbol{V}=\boldsymbol{D}$. Pre and Post multiplying Eq.(2-21) by $\boldsymbol{V}^{T}$ and $\boldsymbol{V}$ respectively yields

$$-\boldsymbol{V}^{T}\boldsymbol{Q}\boldsymbol{V}+\lambda^{*}\boldsymbol{V}^{T}\boldsymbol{I}\boldsymbol{V}=-\boldsymbol{D}+\lambda^{*}\boldsymbol{I}\succeq\boldsymbol{0} \tag{2-22}$$

For the 2-D problem Eq.(2-22) can also be written into its component form

$$-\begin{bmatrix}\lambda_1 & 0\\ 0 & \lambda_2\end{bmatrix}+\begin{bmatrix}\lambda^{*} & 0\\ 0 & \lambda^{*}\end{bmatrix}=\begin{bmatrix}-\lambda_1+\lambda^{*} & 0\\ 0 & -\lambda_2+\lambda^{*}\end{bmatrix}\succeq\boldsymbol{0}$$

Clearly the positive semi-definite condition is equivalent to $-\lambda_1+\lambda^{*}\geq 0$ and $-\lambda_2+\lambda^{*}\geq 0$, or $\lambda^{*}\geq\lambda_1\geq\lambda_2$. It proves that only the largest eigenvalue of $\boldsymbol{Q}$ satisfies the 2nd order condition and hence is the true optimum. In fact $\boldsymbol{H}=-\boldsymbol{Q}+\lambda^{*}\boldsymbol{I}$ can be treated as the Hessian matrix of the Lagrangian in Eq.(2-16) and it would be P.S.D if λ^{*} is the largest eigenvalue of $\boldsymbol{Q}$. According to Theorem 4.8 of [27], the Lagrangian function is convex, and the optimum is global.

The final solution for the Eq.(2-15) problem can therefore be calculated as

$$\left\|\boldsymbol{u}^{j,\Delta f^{1}}\right\|_{\max}^{2}=\left(\Delta\boldsymbol{f}^{1^{*}}\right)^{T}\boldsymbol{Q}\Delta\boldsymbol{f}^{1^{*}}=\left(\Delta\boldsymbol{f}^{1^{*}}\right)^{T}\boldsymbol{V}\boldsymbol{D}\boldsymbol{V}^{T}\Delta\boldsymbol{f}^{1^{*}}=\lambda_{\max}$$

where $\lambda_{\max}$ is the largest eigenvalue of $\boldsymbol{Q}$ and $\Delta\boldsymbol{f}^{1^{*}}$ is the corresponding eigenvector.

2.3.2 Multiple-Uncertainty Problem

In the previous section the simple single uncertainty problem is solved through an eigenvalue approach. The method is extended to a more complicated multiple-uncertainty situation in this section. Considered the Figure 2-9 problem, two uncertain loads are applied with $\boldsymbol{f}^i = \overline{\boldsymbol{f}^i} + \Delta\boldsymbol{f}^i$ and $\overline{\boldsymbol{f}^i} \neq 0$.

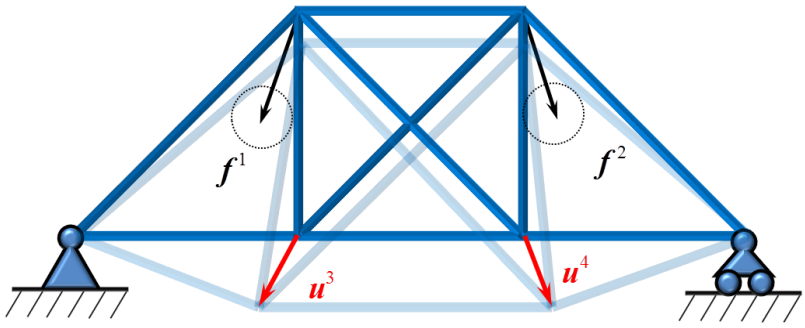

Figure 2-9. The Truss Structure under Multiple Uncertain Loads

The lower level problem is constructed as

$$\begin{aligned} \max_{\boldsymbol{f}^i} \quad & \left\| \boldsymbol{u}^{j,f^1+f^2}(\boldsymbol{f}^1+\boldsymbol{f}^2) \right\|^2 \\ \text{s.t.} \quad & \boldsymbol{f}^1 = \overline{\boldsymbol{f}^1} + \Delta\boldsymbol{f}^1 \\ & \left\| \Delta\boldsymbol{f}^1 \right\|^2 \le 1 \\ & \boldsymbol{f}^2 = \overline{\boldsymbol{f}^2} + \Delta\boldsymbol{f}^2 \\ & \left\| \Delta\boldsymbol{f}^2 \right\|^2 \le 1 \end{aligned} \tag{2-23}$$

Noted that for the linear system $\boldsymbol{u}^{j,f^i}(\boldsymbol{f}^i)$, superposition principle can be applied and the system can be decomposed into $\boldsymbol{u}^{j,f^1+f^2}(\boldsymbol{f}^1+\boldsymbol{f}^2) = \boldsymbol{u}^{j,f^1}(\boldsymbol{f}^1) + \boldsymbol{u}^{j,f^2}(\boldsymbol{f}^2)$, or simply as $\boldsymbol{u}^{j,f^1+f^2} = \boldsymbol{u}^{j,f^1} + \boldsymbol{u}^{j,f^2}$. Utilizing the subadditivity of the norms, an inequality relation can be established as

$$\left\| \boldsymbol{u}^{j,f^1+f^2} \right\| \le \left\| \boldsymbol{u}^{j,f^1} \right\| + \left\| \boldsymbol{u}^{j,f^2} \right\|$$

Take the maximum on both side yields

$$\max\left[\left\|\boldsymbol{u}^{j,f^1+f^2}\right\|\right] \le \max\left[\left\|\boldsymbol{u}^{j,f^1}\right\| + \left\|\boldsymbol{u}^{j,f^2}\right\|\right] \tag{2-24}$$

Since the maximum function is distributive, Eq.(2-24) can be further expanded into

$$\max\left[\left\|\boldsymbol{u}^{j,f^1+f^2}\right\|\right] \le \max\left[\left\|\boldsymbol{u}^{j,f^1}\right\|\right] + \max\left[\left\|\boldsymbol{u}^{j,f^2}\right\|\right] \tag{2-25}$$

Clearly the right hand side of Eq.(2-25) provides a confident bound to the left hand side and can be used as a conservative estimation to the global optimum of the original lower level optimization problem. It also should be noticed that since

$$\begin{aligned} \boldsymbol{f}^i &= \overline{\boldsymbol{f}^i} + \Delta\boldsymbol{f}^i \\ \boldsymbol{u}^{j,\overline{f^i}+\Delta f^i} &= \boldsymbol{u}^{j,\overline{f^i}} + \boldsymbol{u}^{j,\Delta f^i} \end{aligned} \tag{2-26}$$

The inequality relation in Eq.(2-25) can be applied to Eq.(2-26) and yields

$$\max\left[\left\|\boldsymbol{u}^{j,f^i}\right\|\right] = \max\left[\left\|\boldsymbol{u}^{j,\overline{f^i}+\Delta f^i}\right\|\right] \le \left\|\boldsymbol{u}^{j,\overline{f^i}}\right\| + \max\left[\left\|\boldsymbol{u}^{j,\Delta f^i}\right\|\right] \tag{2-27}$$

Recall that the last term in Eq.(2-27) is in face the square root of the objective function of the single uncertainty problem stated Eq.(2-15). Together with the constraint $\left\|\Delta\boldsymbol{f}^i\right\|^2 \le 1$, this term can be calculated as the square root of the solution of the following problem as Eq.(2-28)

$$\begin{aligned} \max_{\Delta\boldsymbol{f}^i} \quad & \left\|\boldsymbol{u}^{j,\Delta f^i}\right\|^2 \\ \text{s.t.} \quad & \left\|\Delta\boldsymbol{f}^i\right\|^2 \le 1 \end{aligned} \tag{2-28}$$

or explicitly expressed as

$$\max\left[\left\|\boldsymbol{u}^{j,\Delta f^i}\right\|\right] = \sqrt{\left(\Delta\boldsymbol{f}^{1*}\right)^T \boldsymbol{Q}_i \Delta\boldsymbol{f}^{1*}} = \sqrt{\lambda_i} \tag{2-29}$$

where λ_i^* is the largest eigenvalue of the corresponding $\boldsymbol{Q}_i$ matrix.

Utilizing the result shown in Eq.(2-29), a conservative bound for the global optimum of the multiple uncertainty problem in Eq.(2-23), namely the Eigenvalue Superposition of Convex Models (ESCM) bound, can be defined as

$$\left\| \boldsymbol{u}^{j,f^1+f^2} \right\|_{\max} = \left\| \boldsymbol{u}^{j,\overline{f}} \right\| + \sqrt{\lambda_1} + \sqrt{\lambda_2} \tag{2-30}$$

This bound can be used as a conservative estimation of the solution of the lower level problem in Eq.(2-7) and by substituting this ESCM bound defined in Eq.(2-30) into the optimization problem stated in Eq.(2-5), the ESCM structure design optimization formulation can be defined, as

$$\begin{aligned} \min_{\boldsymbol{a}} \quad & w = w(\boldsymbol{a}) \\ \text{s.t.} \quad & \left\| \boldsymbol{u}^{j,\overline{f}}(\boldsymbol{a}) \right\| + \sum_{i=1}^{n} \sqrt{\lambda_i(\boldsymbol{a})} \le d_j \end{aligned} \tag{2-31}$$

where $\lambda_i(\boldsymbol{a})$ are the largest eigenvalues of $\boldsymbol{Q}_i(\boldsymbol{a}) = \boldsymbol{A}_i^T \boldsymbol{K}(\boldsymbol{a})^{-T} \boldsymbol{B}_j \boldsymbol{B}_j^T \boldsymbol{K}(\boldsymbol{a})^{-1} \boldsymbol{A}_i$.

2.3.3 Sensitivity Analysis

The sensitivity of the ESCM bound in Eq.(2-31) is calculated in this section. Differentiating the bound with respect to the k^{th} element of the design variable $\boldsymbol{a}$ yields

$$\frac{\partial \left\| \boldsymbol{B}_j^T \boldsymbol{K}^{-1} \overline{\boldsymbol{f}} \right\|}{\partial a_k} + \frac{\partial \left(\sum_i^n \sqrt{\lambda_j} \right)}{\partial a_k} \tag{2-32}$$

The $\partial \left\| \boldsymbol{B}_j^T \boldsymbol{K}^{-1} \overline{\boldsymbol{f}} \right\| / \partial a_k$ term can be calculated as

$$\frac{\partial \left\| \boldsymbol{B}_j^T \boldsymbol{K}^{-1} \overline{\boldsymbol{f}} \right\|}{\partial a_k} = \frac{\partial \sqrt{\overline{\boldsymbol{f}}^T \boldsymbol{K}^{-T} \boldsymbol{B}_j \boldsymbol{B}_j^T \boldsymbol{K}^{-1} \overline{\boldsymbol{f}}}}{\partial a_k} = \left(\frac{1}{2\sqrt{\overline{\boldsymbol{f}}^T \boldsymbol{K}^{-T} \boldsymbol{B}_j \boldsymbol{B}_j^T \boldsymbol{K}^{-1} \overline{\boldsymbol{f}}}} \right) \frac{\partial \left(\overline{\boldsymbol{f}}^T \boldsymbol{K}^{-T} \boldsymbol{B}_j \boldsymbol{B}_j^T \boldsymbol{K}^{-1} \overline{\boldsymbol{f}} \right)}{\partial a_k}$$

where

$$\frac{\partial\left(\overline{\boldsymbol{f}}^T \boldsymbol{K}^{-T} \boldsymbol{B}_j \boldsymbol{B}_j^T \boldsymbol{K}^{-1} \overline{\boldsymbol{f}}\right)}{\partial a_k} = \overline{\boldsymbol{f}}^T \boldsymbol{K}^{-T} \boldsymbol{B}_j \boldsymbol{B}_j^T \frac{\partial \boldsymbol{K}^{-1}}{\partial a_k} \overline{\boldsymbol{f}} + \left(\overline{\boldsymbol{f}}^T \boldsymbol{K}^{-T} \boldsymbol{B}_j \boldsymbol{B}_j^T \frac{\partial \boldsymbol{K}^{-1}}{\partial a_k} \overline{\boldsymbol{f}}\right)^T$$

$$\frac{\partial \boldsymbol{K}^{-1}}{\partial a_k} = -\boldsymbol{K}^{-1} \frac{\partial \boldsymbol{K}}{\partial a_k} \boldsymbol{K}^{-1}$$

For the $\partial\left(\sum_i^n \sqrt{\lambda_j}\right)\Big/\partial a_k$ term, it can be expanded into

$$\frac{\partial\left(\sum_i^n \sqrt{\lambda_j}\right)}{\partial a_k} = \left(\sum_i^n \frac{1}{2\sqrt{\lambda_i}} \frac{\partial \lambda_i}{\partial a_k}\right)$$

the $\partial\lambda_i/\partial a_k$ term involves eigenvalue differentiation and in case of none repeating eigenvalue, the Nelson's method[28] can be used and the result is given as

$$\frac{\partial \lambda_i}{\partial a_k} = \boldsymbol{x}^T \frac{\partial \boldsymbol{Q}_i}{\partial a_k} \boldsymbol{x}$$

where $\boldsymbol{x}$ is the eigenvector corresponding to the largest eigenvalue λ_i. The $\partial \boldsymbol{Q}_i/\partial a_k$ term is derived following the chain rule

$$\frac{\partial \boldsymbol{Q}_i}{\partial a_k} = -[\boldsymbol{A}_i^T \boldsymbol{K}^{-T} \boldsymbol{B}_j \boldsymbol{B}_j{}^T \boldsymbol{K}^{-1} \frac{\partial \boldsymbol{K}}{\partial a_k} \boldsymbol{K}^{-1} \boldsymbol{A}_i + \left(\boldsymbol{A}_i^T \boldsymbol{K}^{-T} \boldsymbol{B}_j \boldsymbol{B}_j{}^T \boldsymbol{K}^{-1} \frac{\partial \boldsymbol{K}}{\partial a_k} \boldsymbol{K}^{-1} \boldsymbol{A}_i\right)^T]$$

For the repeating eigenvalue problem, other methods such as given in [29, 30] can be employed, and that completes the sensitivity analysis.

2.4 Numerical Examples

Two numerical examples are presented in this section. In the first example, a simple truss design with one uncertain external load is solved. In the second example, a multiple external loads with uncertainties case is considered. The results from the

proposed ESCM method are compared to those from SDP method and Monte Carlo simulation.

2.4.1 Single Load with Uncertainty

Consider the 4-node 5-element truss structure with 1 external load. The initial structure configuration is given in Figure 2-10. Node 1 and Node 2 are fixed in both horizontal and vertical directions. The load with uncertainties is applied at Node 3.

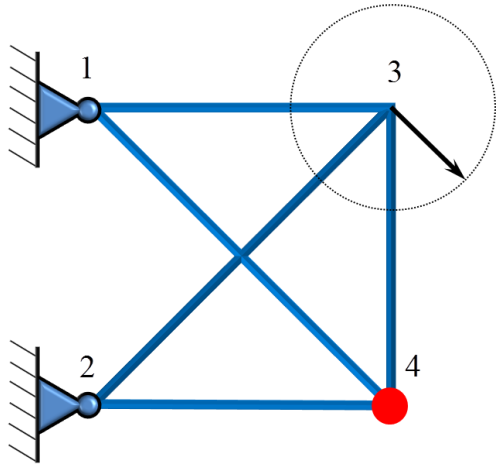

Figure 2-10. The 4-Node 5-Element Truss Structure

The total weight of the structure is minimized subject to the constraint that the magnitude of displacement of Node 4 to be smaller or equal to 0.5. The Young's modulus E and density ρ are 10 and 1 respectively for all elements. The external loads with uncertainties are modeled in the circle unknown-but-bounded model. Their nominal value $\overline{f}$ is zero. The deviation Δf is described as

$$\left|\Delta \boldsymbol{f}\right|^2 = \Delta \boldsymbol{f}^T \Delta \boldsymbol{f} = \Delta \boldsymbol{f}^T \boldsymbol{A}\boldsymbol{A}^T \Delta \boldsymbol{f} \le 1$$

The mathematical formulation of the this truss design problem is constructed as

$$\begin{aligned} \min_{\boldsymbol{a}} \quad & w = w(\boldsymbol{a}) = \sum_m \rho_m l_m a_m \\ \text{s.t.} \quad & \boldsymbol{f} = \Delta \boldsymbol{f} \\ & \left|\Delta \boldsymbol{f}\right|^2 = \Delta \boldsymbol{f}^T \Delta \boldsymbol{f} = \Delta \boldsymbol{f}^T \boldsymbol{A}\boldsymbol{A}^T \Delta \boldsymbol{f} \le 1 \\ & \max_{\boldsymbol{f}}[\left|\boldsymbol{u}^4(\boldsymbol{a}, \boldsymbol{f})\right|] \le 0.5 \\ & \boldsymbol{a} \in (\boldsymbol{0.1}, \boldsymbol{300}) \end{aligned} \tag{2-33}$$

The ESCM bound and the SDP bound are evaluated at $\boldsymbol{a} = \boldsymbol{0.5}$ to exam their effectiveness.

Table 2-1. Function Value when $a = 0.5$ for Example 1

	Function Value	Difference	Relative Diff
Monte Carlo	0.3617		
SDP	0.3617	0	0%
ESCM	0.3617	0	0%

As seen in Table 2-1, the results from both the ESCM and SDP methods match with the result form Monte Carlo simulation, which is considered as the true solution. The yalmip [31] SDP solver converges to its solution in 6 iterations. The time cost for both methods in this example are similar. The results prove the derivations in section 2.3.1, that the ESCM method solves the single-constraint QCQP problem to its global optimum. The SDP method also gives the exact solution in this situation, as proven by Boyd [32].

The SDP relaxation formulation and the ESCM single level formulation are solved by the fmincon function using interior-point algorithm respectively. For the SDP problem, the gradient of the objective function is user-provided, while the gradient of the constraint is approximated by FDM, since the explicit expression of the gradient of the SDP bound cannot be derived. For the ESCM problem, the gradients of the objective

function and the constraint are analytically calculated and they are verified by the DerivativeCheck option in fmincon with central difference FDM. At the point $\boldsymbol{a} = 0.5$, the maximum relative discrepancies between analytic solution and FDM are 2.36×10^{-11} for the objective function and 2.51×10^{-14} for the constraint. Both problems converge to their local optima and the results are listed in Table 2-2.

Table 2-2. Results from SDP and ESCM for Example 1

	Optimum Func Value	Iterations	Func Calls
SDP	1.5168	26	162
ESCM	1.5167	20	22

The ESCM demonstrates a significantly higher efficiency and produces a slightly better result compare to the SDP. Because of the FDM, the number of function calls in the SDP is high. The large amount of function calls greatly impact the efficiency of the SDP approach. The optimized elements sizes are listed in Table 2-3.

Table 2-3. ESCM Optimized Elements Sizes of Example 1

$\boldsymbol{a}_i$	1	2	3	4	5
SDP	0.2678	0.3115	0.2678	0.1000	0.3115
ESCM	0.2678	0.3115	0.2678	0.1000	0.3115

At the accuracy of 4 significant digits, the optimized configuration of the SDP and ESCM are the same. The optimized configuration is plotted in Figure 2-11.

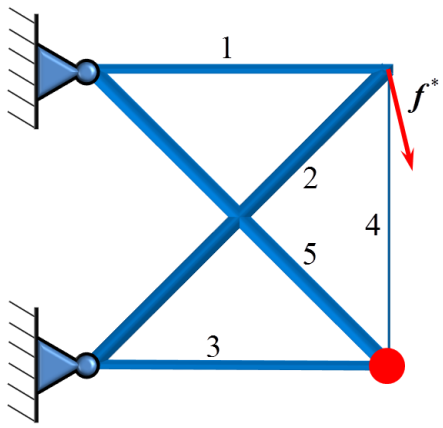

Figure 2-11. Optimized Structure Configuration of Example 1

The structure could be viewed as two independent triangles linked by one bar. The upper triangle is formed by element 1 and 2 while element 3 and 5 form up the lower triangle. They are connected by element 4. The upper triangle supports the load hence it is strengthened by the optimizer. The displacement is measured at the lower triangle so it is also reinforced. The connection between the two triangles is set to the lower bound hence minimum amount of force is transferred. The optimized configuration is verified by Monte Carlo simulation and the results are shown in Table 2-4.

Table 2-4. Verification of the Optimized Result for Example 1

	Function Value	Difference	Relative Diff
Monte Carlo	0.5		
ESCM	0.5	0	0%

The ESCM produces the exact solution as expected.

It is observed in the first example that since both the ESCM and SDP methods give the exact solutions for the single-constraint lower level sub problem, the ESCM

design and SDP design converge to the same optimized configuration. Thanks to the simplicity and differentiability of the ESCM bound, the ESCM single level formulation converges in less iteration and makes fewer function calls comparing to the SDP two-level approach.

2.4.2 Multiple Loads with Uncertainties

To demonstrate the effectiveness of the proposed ESCM method, a truss structure design optimization problem with multiple uncertain loads is examined. The structure is composed of 9 nodes and 16 elements, as shown in Figure 2-12. Node 1 and Node 2 are fixed in both directions and loads are applied to all other nodes. In this problem, the design variable is the element cross section area vector $\boldsymbol{a}$ and the total weight of the structure is minimized subject to the constraint that the maximum magnitude of displacement of Node 9 to be smaller or equal to 0.5. The Young's modulus E and density ρ are 100 and 1 respectively for all elements. The external loads with uncertainties are modeled in the unknown-but-bounded model. The nominal value vector $\bar{\boldsymbol{f}}$ is listed in Table 2-5.

Table 2-5. The Value for the Nominal Load Vector $\bar{\boldsymbol{f}}$

i	3	4	5	6	7	8	9
$\overline{\boldsymbol{f}_x^i}$	0	0	0	0	0	0	0
$\overline{\boldsymbol{f}_y^i}$	-2	-2	-2	-2	-2	-2	-2

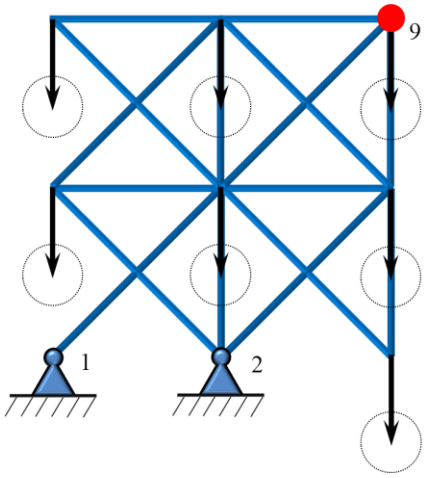

Figure 2-12. The 9-Node 16-Element Truss Structure

The ESCM single level optimization problem is formulated as follow

$$\begin{aligned} \min_{\boldsymbol{a}} \quad & w = w(\boldsymbol{a}) = \sum_m \rho_m l_m a_m \\ \text{s.t.} \quad & \left\| \boldsymbol{u}^{9,f^i}\left(\boldsymbol{a}, \boldsymbol{f}^i\right) \right\|_{\max} \le 0.5 \\ & \boldsymbol{f}^i = \overline{\boldsymbol{f}^i} + \Delta \boldsymbol{f}^i \\ & \left\| \Delta \boldsymbol{f}^i \right\|^2 \le 1 \\ & \boldsymbol{a} \in (\boldsymbol{0.1}, \boldsymbol{300}) \end{aligned} \tag{2-34}$$

The ESCM bound and the SDP bound are evaluated at $\boldsymbol{a} = 1$ to exam their effectiveness. Since this is a multiple uncertainty problem, both methods give conservative estimations of the true solution, as shown in Table 2-6.

Table 2-6. Function Value when $\boldsymbol{a}^0 = \boldsymbol{1}$

	Function Value	Difference	Relative Diff
Monte Carlo	1.6125		
ESCM	1.6546	0.0421	2.6%
SDP	1.6489	0.0364	2.3%

The Eq.(2-34) problem is solved using the ESCM method. The algorithm consistently converged to the same solution from different starting points; and since the 1st order optimality conditions are satisfied for all the trials, the solution is indeed the optimum solution. The details are shown in Table 2-7 and it is demonstrated in this example that the ESCM single level formulation provides an efficient and stable approach for solving the truss design optimization problem.

Table 2-7. ESCM Results from Different Starting Point

Starting Point	Optimum Func Value	1st Order Optimality	Iteration	Func Calls
$\boldsymbol{a^0 = 300}$	20.2708	1.280×10^{-6}	55	59
$\boldsymbol{a^0 = 1}$	20.2708	1.280×10^{-6}	32	37
$\boldsymbol{a^0 = 0.5}$	20.2708	1.280×10^{-6}	38	45
$\boldsymbol{a^0 = 0.01}$	20.2708	1.280×10^{-6}	34	35

The optimized elements sizes are listed in Table 2-8. All none listed elements sizes are set to the lower bound, which is 0.1, by the optimizer.

Table 2-8. ESCM Optimized Elements Sizes

i	1	3	4	5	7	13	14	16
$\boldsymbol{a}_i$	4.6362	0.1003	3.0758	3.1025	2.3990	0.9322	0.2332	1.1376

The optimized configuration is verified by Monte Carlo simulation and is considered as a safe design. The results are shown in Table 2-9.

Table 2-9. Verification of the Optimized

	Function Value	Difference	Relative Diff
Monte Carlo	0.4704		
ESCM	0.5	0.0296	6.3%

As a comparison the SDP relaxation method is also used to solve the Eq.(2-34) problem. Multiple starting points had been tried and the algorithm stopped at different points. A significantly higher number of iterations and function calls compare to the ESCM method is observed and the 1st order optimality conditions are not satisfied hence the solutions are feasible solutions instead of optimum solutions. When starting from infeasible domain, i.e., $\boldsymbol{a}^0 = 0.01$, the program terminated after 8 iterations reporting no feasible solution found. The results are listed in Table 2-10 and one can reach the conclusions from this example that the SDP relaxation formulation is very sensitive to staring point and is low in efficiency.

Table 2-10. SDP Relaxation Results from Different Starting Point

Starting Point	Optimum Func Value	1st Order Optimality	Step Size	Iter	Func Calls
$\boldsymbol{a}^0 = 300$	19.1240	1.412	5.85×10^{-11}	110	2034
$\boldsymbol{a}^0 = 1$	19.8154	31810	5.67×10^{-11}	76	1431
$\boldsymbol{a}^0 = 0.5$	19.8117	30050	8.64×10^{-11}	19	354
$\boldsymbol{a}^0 = 0.01$	N/A	N/A	N/A	8	159

From the results of this example it could be seen that both the ESCM and the SDP conservatively estimate the global optimum of the multiple-constraint lower level

problem. The SDP approach fails to give an optimum solution from multiple starting points. On the other hand the ESCM single level formulation converges significantly faster than the SDP relaxation formulation and stably reaches the same optimum solution from a different starting point. As verified by the Monte Carlo simulation, the ESCM approach gives a safe design.

Chapter 3

Convex Modeling Based Topology Optimization

Topology optimization is an optimization method which finds material distribution that optimizes an objective function while satisfying certain constraints within the predefined design domain. Ever since the introduction of the homogenization method by Bendsøe and Kikuchi[33] into structural topology optimization problems, the topology optimization of solid continuum has become one of the most active fields in structural design optimization community during the past few decades.

3.1 Introduction to Topology Optimization Method

In order to formulate the topology optimization problem, the design variable, the objective function and the constraints need to be defined. In a typical topology optimization problem, the design variable is the material distribution described by $\boldsymbol{a}$ and the problem can be presented as

$$\min_{\boldsymbol{a}} \quad \int_\Omega \phi(\boldsymbol{a})\, d\Omega \tag{3-1}$$

$$\text{s.t.} \quad \int_\Omega \rho(\boldsymbol{a})\, d\Omega \le V_0 \tag{3-2}$$

$$\boldsymbol{a} \in \{0,1\} \tag{3-3}$$

$$\begin{aligned} \nabla \cdot \boldsymbol{\sigma} + \boldsymbol{f} &= \boldsymbol{0} \\ \boldsymbol{\sigma} &= \boldsymbol{C} : \boldsymbol{\varepsilon} \end{aligned} \tag{3-4}$$

The objective function in Eq.(3-1) measures the performance of the structure. The $\phi(\boldsymbol{a})$ term is the structure property function and many different types of properties can be used as the objective, including the most commonly accepted strain energy. The inequality relation described in Eq.(3-2) limits the total material usage with the $\rho(\boldsymbol{a})$ term as the material density function. Equation Eq.(3-3) indicates that the design variable has to take the value 1 by selection and 0 by de-selection at any point within the domain. Finally the behavior of the structure is governed by the PDE system stated in Eq.(3-4). Analytical solution of PDEs of complex systems are sometimes unavailable and often impractical to calculate, finite element analysis is usually involved. Consequently the general formulation can be expressed as (assuming strain energy is used as the objective function)

$$\begin{aligned} \min_{\boldsymbol{a}} \quad & U = \boldsymbol{u}^T \boldsymbol{K} \boldsymbol{u} \\ \text{s.t.} \quad & \int_\Omega \rho(\boldsymbol{a})\, d\Omega = \sum_{i=1}^{N} a_i v_i \le V_0 \\ & \boldsymbol{a} \in \{0,1\} \\ & \boldsymbol{K}\left(\rho(\boldsymbol{a})\right)\boldsymbol{u} = \boldsymbol{f} \end{aligned} \tag{3-5}$$

Here v_i represents the volume of the i^{th} element of the meshed domain and the material usage is calculated through summation of all the selected elements, which is defined by the value of a_i, the volume integral over the domain is thus simplified due to the discretization. The behavior of the system is described by the stiffness matrix $\boldsymbol{K}$, which is a function of the material density $\rho(\boldsymbol{a})$, and the force vector $\boldsymbol{f}$.

Clearly the problem stated in Eq.(3-5) is a binary optimization problem since the design value is restricted to take either 1 or 0. Generally, the solution to such

optimization problem is not yet practicable. Therefore continuous optimization strategies, such as methods based on the Solid Isotropic Material with Penalization (SIMP) model [34] are often adopted where the material density is assumed to vary from 0 to 1, or $\boldsymbol{0 \le a \le 1}$.

The SIMP model describes the material in the following way:

$$\boldsymbol{K}_e(a) = \rho(a)^p \boldsymbol{K}_e^0 \tag{3-6}$$

where $\boldsymbol{K}_e$ is the element stiffness matrix and $\boldsymbol{K}_e^0$ defines the material properties of a given isotropic material. Clearly $\boldsymbol{K}_e(\rho = 0) = 0$ and $\boldsymbol{K}_e(\rho = 1) = \boldsymbol{K}_e^0$, and the model described in Eq.(3-6) interpolates between the material properties 0 and $\boldsymbol{K}_e^0$. When specifying the penalty parameter $p > 1$, the SIMP model makes the intermediate densities unfavorable therefore a 0-1 design can be obtained. The effect of different penalty is illustrated in Figure 3-1. Usually $p = 3$ is selected [35].

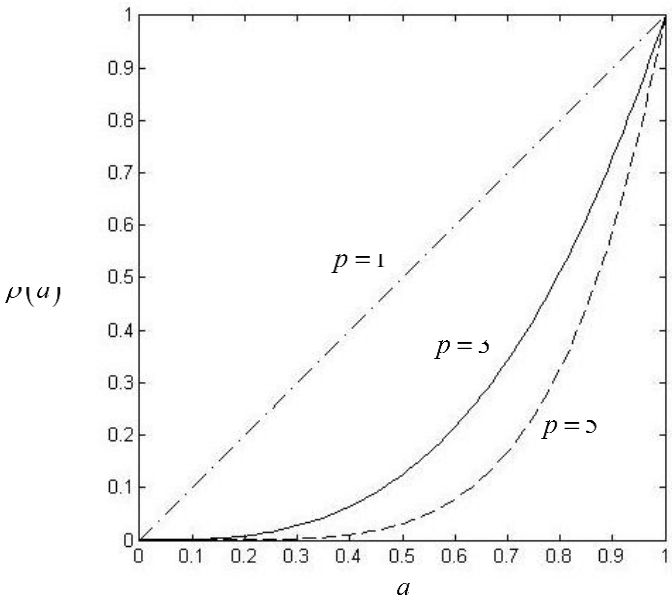

Figure 3-1 SIMP Model with Different Penalty

Following this idea the problem formulation is evolved into

$$\begin{aligned} \min_{\boldsymbol{a}} \quad & U = \boldsymbol{u}^T \boldsymbol{K}\boldsymbol{u} \\ \text{s.t.} \quad & \sum_{i=1}^{N} a_i v_i \le V_0 \\ & \boldsymbol{0} \le \boldsymbol{a} \le \boldsymbol{1} \\ & \boldsymbol{K}_e = \rho^3 \boldsymbol{K}_e^0 \\ & \boldsymbol{K}\boldsymbol{u} = \boldsymbol{f} \end{aligned} \tag{3-7}$$

In the problem showed in Eq.(3-7) the objective function and the constraints are continuous and differentiable, and therefore the optimization problem can be solved using gradient based optimization algorithms. The material density of each element is updated using the sensitivity information during the optimization process and the optimization algorithm eventually finds the optimal structure. The flow chart for solving the topology optimization problems is illustrated in Figure 3-2.

For conciseness some constraints in Eq.(3-7) are deliberately hidden and this simplification yields

$$\begin{aligned} \min_{\boldsymbol{a}} \quad & U = \boldsymbol{u}^T \boldsymbol{K}\boldsymbol{u} \\ \text{s.t.} \quad & \boldsymbol{K}\boldsymbol{u} = \boldsymbol{f} \\ & V = \sum_{i=1}^{N} a_i v_i \le V_0 \end{aligned} \tag{3-8}$$

It should be kept in mind that although not shown in the problem statement, the system is still subject to those constraints.

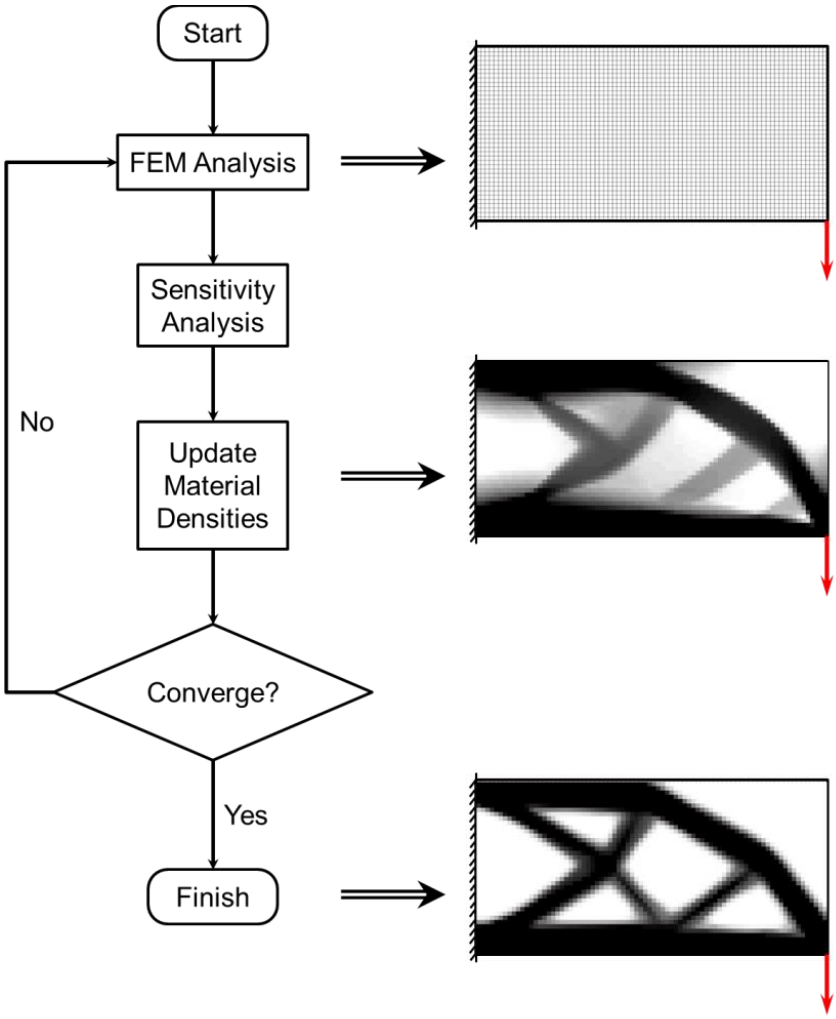

Figure 3-2 The Workflow of Topology Optimization

3.1.1 Strain Based Topology Optimization Method

Although widely accepted the strain energy based topology optimization formulation has its limitations. Introduced by Lee [36], the strain based topology optimization method resolves the problems of strain distortion and stress concentration of the traditional method. In this new method the objective function is defined in terms of the effective strain $\bar{\varepsilon}$, as shown in Eq.(3-9).

$$\begin{aligned} \min_{\boldsymbol{a}} \quad & \sum_{i=1}^{N} \bar{\varepsilon}_i^2 \\ \text{s.t.} \quad & \boldsymbol{K}\boldsymbol{u} = \boldsymbol{f} \\ & V \le V_0 \end{aligned} \tag{3-9}$$

The square of effective strain of the i^{th} element $\bar{\varepsilon}_i^2$ can be calculated as:

$$\bar{\varepsilon}^2 = \boldsymbol{u}_e^T \boldsymbol{C} \boldsymbol{u}_e = \frac{\boldsymbol{u}_e^T \boldsymbol{K}_e \boldsymbol{u}_e}{\rho(a) E^0} = \frac{\boldsymbol{u}_e^T \boldsymbol{K}_e^0 \boldsymbol{u}_e}{E^0} \tag{3-10}$$

where $\boldsymbol{C}$ is the stress strain relation matrix; $\boldsymbol{K}_e^0$ is the element stiffness matrix without the material density function $\rho(a)^p$, as in Eq. (3-6); and E^0 is the base Young's modulus.

By defining the new global stiffness matrix $\boldsymbol{K}^0$ assembled from $\boldsymbol{K}_e^0 / E^0$, the topology optimization problem in Eq.(3-9) can be rewritten as

$$\begin{aligned} \min_{\boldsymbol{a}} \quad & \sum_{i=1}^{N} \bar{\varepsilon}_i^2 = \boldsymbol{u}^T \boldsymbol{K}^0 \boldsymbol{u} \\ \text{s.t.} \quad & \boldsymbol{K}\boldsymbol{u} = \boldsymbol{f} \\ & V \le V_0 \end{aligned} \tag{3-11}$$

The effectiveness of the strain based topology optimization method can be seen from the following example given by Lee [36]:

Consider the cantilever problem defined in Figure 3-3:

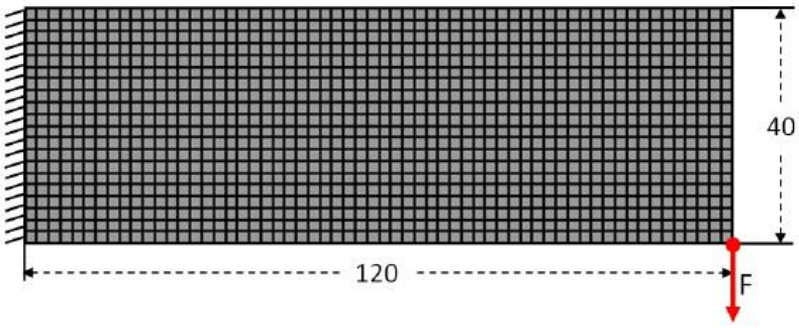

Figure 3-3 Problem Definition for the Strain Based Method Example[2]

[2] Resource: 36. Lee, E. and Rutgers University. Graduate School--New Brunswick., *A strain based topology optimization method*, 2011. p. x, 112 p.

The beam has its left edge fixed and a vertical force is applied at the lower right corner. The problem is also solved using the traditional strain energy based formulation as comparison. The optimum design configurations are plotted in Figure 3-4 and in Figure 3-5 the Von Mises Stress is plotted for both designs. It proves that compared to the traditional strain energy based method, high stress concentration can be avoided in the strain based topology optimization method.

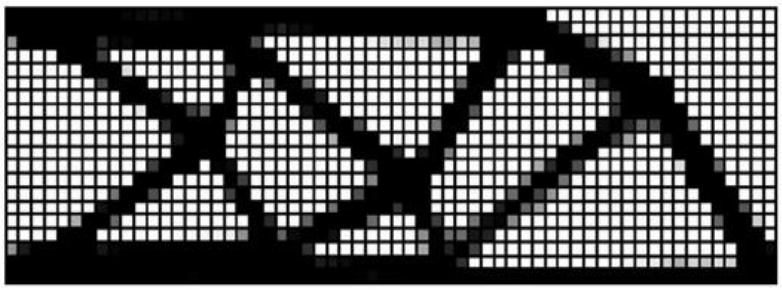

(a) Strain Based Formulation

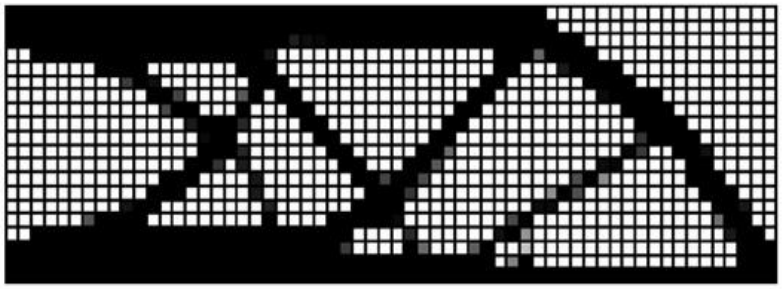

(b) Strain Energy Based Formulation

Figure 3-4 Results of the Strain Based Method Example[3]

[3] Resources: 36. Ibid.

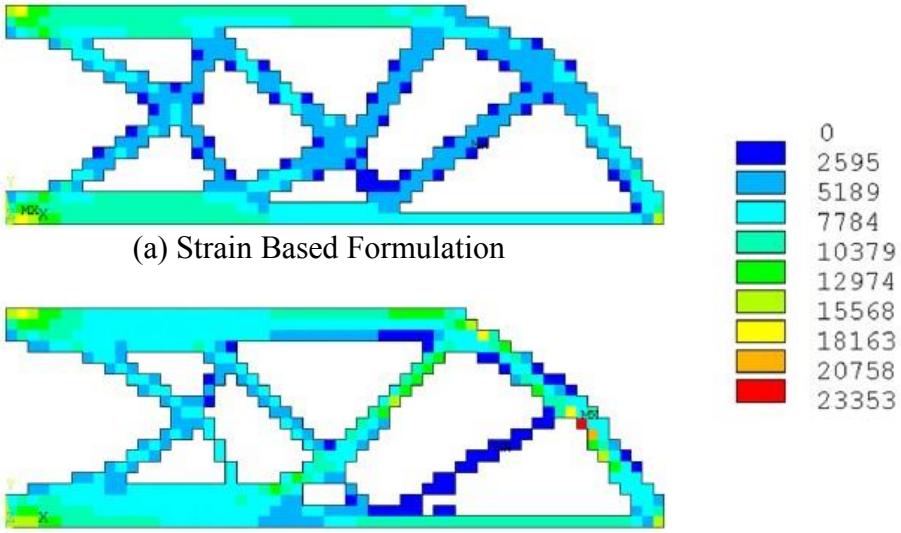

(a) Strain Based Formulation

(b) Strain Energy Based Formulation

Figure 3-5 Von Mises Stress Plot of the Strain Based Method Example[4]

3.2 Topology Optimization under Load Uncertainty

In the traditional topology optimization formulation all the parameters, for example the external excitations, are often assumed to be deterministic. However in practical applications uncertainties are always unavoidable. Measurement errors, inaccuracy in manufacturing process, perturbations in external environment for example, are possible sources of uncertainties. The introduction of uncertainties not only affects the reliability of the final design but can also dramatically change the overall structure layout in certain circumstances [37], therefore the uncertainties must be considered in the design problem in order to achieve a more reliable solution.

[4] Resource: 36. Ibid.

Many methods has been developed to tackle such problems, for example, the Reliability Based Topology Optimization (RBTO) is proposed by Kharmand and Olhoff [37]. This approach has attracted a lot of attention and led to many studies of the kind. For example the three-dimensional geometrical nonlinearity problem solved by Jung and Cho [38] utilized the RBTO framework. Ayyub systematically studied the application of fuzzy sets concept in structural design [39] and the object in the design was described by a fuzzy set. However as discussed in Chapter 1, the probabilistic based method requires extensive statistical information on the uncertain parameter, and the fuzzy set based methods has their own disadvantages, such as complexity when multiple variables presented [40]. Based on the worst case design optimization (also called anti-optimization) concept introduced by Elishakoff in [41], a method utilizing genetic algorithm (GA) was proposed by Venter and Haftka in [42], which reduced the two-level optimization problem into a single level problem. In this research, the topology optimization problem under external load uncertainty is constructed following the convex model and utilizing the worst case design optimization concept. To illustrate the solution strategy to this problem, an example shown in Figure 3-6 is used.

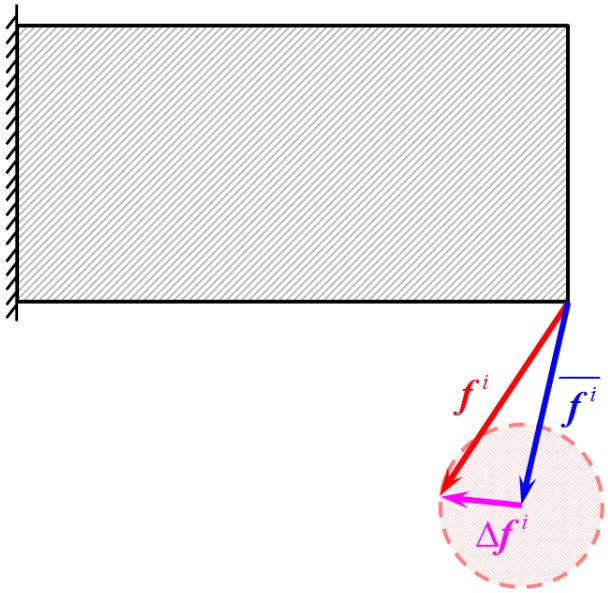

Figure 3-6 Topology Optimization under Load Uncertainty

In this problem, the load uncertainty is formulated following the same unknown-but-bounded model as describe in section 2.3, which decomposes the load into the nominal part and perturbation part, and the magnitude of the perturbation is bounded. Mathematically this model is expressed as

$$\boldsymbol{f}^i = \overline{\boldsymbol{f}^i} + \Delta\boldsymbol{f}^i$$
$$\left\|\Delta\boldsymbol{f}^i\right\|^2 = \left(\Delta\boldsymbol{f}^i\right)^T \Delta\boldsymbol{f}^i \le \sqrt{c^2}$$

The $\overline{\boldsymbol{f}^i}$ represents the nominal load and $\Delta\boldsymbol{f}^i$ denotes the perturbation. The design target is to find the optimum material distribution which minimizes the total strain energy of the structure. However the introduction of load uncertainty into the original problem would render the objective, i.e., the strain energy, which is a function of the load, undeterministic. By the spirit of worst case scenario design, the maximum possible strain energy under the given uncertain load is selected as the new objective in order to achieve a conservative, or safe, solution. Thus the problem shown in Figure 3-6 can be described

as an optimization problem to find the optimum material distribution that minimizes the maximum possible strain energy under the load uncertainty.

3.2.1 Problem Formulation

Following the previous argument and introducing the load uncertainty into the design problem in Eq. (3-8), the formulation for the problem in Figure 3-6 is established as

$$\begin{aligned} \min_{\boldsymbol{a}} \quad & U_{\max} = \left(\boldsymbol{u}^T \boldsymbol{K}\boldsymbol{u}\right)_{\max} \\ \text{s.t.} \quad & \boldsymbol{K}\boldsymbol{u} = \boldsymbol{f} \\ & V \le V_0 \\ & \boldsymbol{f} = \boldsymbol{A}\boldsymbol{f}^i \\ & \boldsymbol{f}^i = \overline{\boldsymbol{f}^i} + \Delta\boldsymbol{f}^i \\ & \left(\Delta\boldsymbol{f}^i\right)^T \Delta\boldsymbol{f}^i \le \sqrt{c^2} \end{aligned} \tag{3-12}$$

The maximum value of the objective function can be found through solving the lower level optimization problem, which is defined as

$$\begin{aligned} \max_{\boldsymbol{f}} \quad & U = \boldsymbol{u}^T \boldsymbol{K}\boldsymbol{u} \\ \text{s.t.} \quad & \boldsymbol{K}\boldsymbol{u} = \boldsymbol{f} \\ & \boldsymbol{f} = \boldsymbol{A}\boldsymbol{f}^i \\ & \boldsymbol{f}^i = \overline{\boldsymbol{f}^i} + \Delta\boldsymbol{f}^i \\ & \left(\Delta\boldsymbol{f}^i\right)^T \Delta\boldsymbol{f}^i \le \sqrt{c^2} \end{aligned} \tag{3-13}$$

Consequently the Eq. (3-12) upper level problem can be simplified into

$$\begin{aligned} \min_{\boldsymbol{a}} \quad & U_{\max}\left(\boldsymbol{a}\right) \\ \text{s.t.} \quad & V\left(\boldsymbol{a}\right) \le V_0 \end{aligned} \tag{3-14}$$

with $U_{\max}$ term being the global optimum solution of the lower level problem states Eq.(3-13). Now the solution process of the design problem relies on the success in

evaluating the objective function value and more importantly its sensitivity with respect to the design variable, that is, calculating $U_{\max}(\boldsymbol{a})$ and the sensitivity term $\partial U_{\max}(\boldsymbol{a})/\partial a_k$.

Since the objective $U_{\max}$ is the solution of the problem in Eq.(3-13), evaluating its value is in fact equivalent to solving the lower level optimization problem to its global maximum solution. Using equality constraints $\boldsymbol{Ku}=\boldsymbol{f}$, $\boldsymbol{f}=\boldsymbol{Af}^i$ and $\boldsymbol{f}=\overline{\boldsymbol{f}}+\Delta\boldsymbol{f}$ of Eq.(3-13) in the expression of the objective $U=\boldsymbol{u}^T\boldsymbol{f}$, the problem can be rewritten as

$$\begin{aligned} \max \quad & \left(\overline{\boldsymbol{f}^i}+\Delta\boldsymbol{f}^i\right)^T\boldsymbol{Q}\left(\overline{\boldsymbol{f}^i}+\Delta\boldsymbol{f}^i\right) \\ \text{s.t.} \quad & \left(\Delta\boldsymbol{f}^i\right)^T\Delta\boldsymbol{f}^i\le 1 \end{aligned} \tag{3-15}$$

where $\boldsymbol{Q}=\boldsymbol{A}^T\boldsymbol{KA}$ and $\boldsymbol{Q}$ is Positive Semi-Definite (P.S.D) and for simplicity the constraint is assumed to be $\left(\Delta\boldsymbol{f}^i\right)^T\Delta\boldsymbol{f}^i\le 1$ instead of $\left(\Delta\boldsymbol{f}^i\right)^T\Delta\boldsymbol{f}^i\le\sqrt{c^2}$. The feasible domain of the problem in Eq.(3-15) is plotted in Figure 3-7.

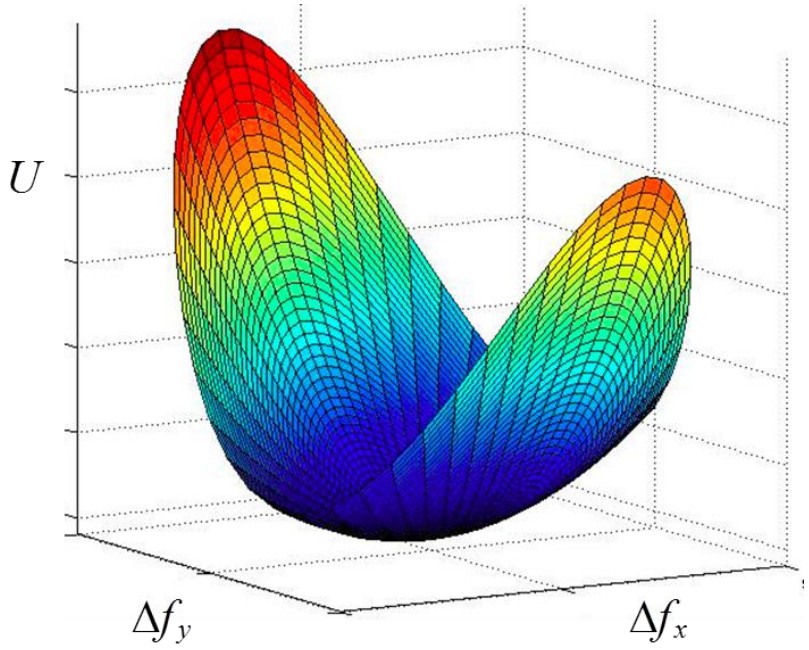

Figure 3-7 Feasible Domain of Eq.(3-15) Problem

Clearly the problem is concave since the existence of multiple local maxima is observed. Therefore solving this problem using a conventional gradient based method may lead to different local optima when searching from different starting point and consequently the true worst case situation cannot be reliably identified. Furthermore using a time consuming iterative method for this lower level problem would make solving the already computational intense upper level topology optimization problem impractical, since the lower level problem needs to be solved in every iteration of the upper level design process.

3.3 Convex Modeling Based Topology Optimization

In order to overcome the aforementioned challenges the convex modeling based topology optimization method is developed from the ESCM method. Firstly the lower level problem, which is to identify the worst case structure response, is solved; the sensitivity of the lower level solution is then analyzed. With the function value and sensitivity information ready, the upper level design problem can be solved through a gradient based topology optimization algorithm.

3.3.1 Solution and Sensitivity of the Lower Level Problem

Following the concepts of the ESCM method, the solution strategy starts with analyzing the KKT optimality conditions. The Lagrangian of the problem in Eq.(3-15) can be found as

$$\begin{aligned} L &= -\left(\overline{\boldsymbol{f}^i} + \Delta\boldsymbol{f}^i\right)^T \boldsymbol{Q}\left(\overline{\boldsymbol{f}^i} + \Delta\boldsymbol{f}^i\right) + \lambda\left[\left(\Delta\boldsymbol{f}^i\right)^T \Delta\boldsymbol{f}^i - 1\right] \\ &= -\left(\Delta\boldsymbol{f}^i\right)^T \boldsymbol{Q}\Delta\boldsymbol{f}^i - 2\left(\Delta\boldsymbol{f}^i\right)^T \boldsymbol{Q}\,\overline{\boldsymbol{f}^i} - \left(\overline{\boldsymbol{f}^i}\right)^T \boldsymbol{Q}\,\overline{\boldsymbol{f}^i} + \lambda\left[\left(\Delta\boldsymbol{f}^i\right)^T \Delta\boldsymbol{f}^i - 1\right] \end{aligned} \tag{3-16}$$

The 1st order KKT conditions are established from differentiating the Lagrangian:

$$\frac{dL}{d\Delta\boldsymbol{f}^i} = -2\boldsymbol{Q}\Delta\boldsymbol{f}^i - 2\boldsymbol{Q}\,\overline{\boldsymbol{f}^i} + 2\lambda\Delta\boldsymbol{f}^i = \boldsymbol{0} \tag{3-17}$$

$$\left(\Delta\boldsymbol{f}^i\right)^T \Delta\boldsymbol{f}^i - 1 \le 0 \tag{3-18}$$

$$\lambda \ge 0 \tag{3-19}$$

$$\lambda\left[\left(\Delta\boldsymbol{f}^i\right)^T \Delta\boldsymbol{f}^i - 1\right] = 0 \tag{3-20}$$

Differentiating the Lagrangian one more time yields the 2nd order condition:

$$\frac{d^2L}{d\left(\Delta\boldsymbol{f}^i\right)^2} = -2\boldsymbol{Q} + 2\lambda\boldsymbol{I} \succeq \boldsymbol{0} \tag{3-21}$$

It should be noted that the 2nd order condition in Eq.(3-21) requires $\lambda \ge \lambda_1$, where λ_1 is the largest eigenvalue of $\boldsymbol{Q}$ and $\lambda_1 > 0$. Together with the complementary slackness condition in Eq.(3-20) it could be proven that the inequality constraint in Eq.(3-18) must be active at the global optimum, therefore it can be treated as an equality constraint

$$\left(\Delta\boldsymbol{f}^i\right)^T \Delta\boldsymbol{f}^i - 1 = 0 \tag{3-22}$$

Rearranging the terms in the stationarity condition in Eq.(3-17) yields

$$-\boldsymbol{Q}\Delta\boldsymbol{f}^i - \boldsymbol{Q}\overline{\boldsymbol{f}^i} + \lambda\Delta\boldsymbol{f}^i = \boldsymbol{0} \tag{3-23}$$

Since matrix $\boldsymbol{Q}$ is symmetric by construction, it is never defective and always has a complete basis of eigenvectors, hence can be decomposed using the eigen-decomposition, which yields $\boldsymbol{Q} = \boldsymbol{V}\boldsymbol{D}\boldsymbol{V}^T$. Pre-multiplying Eq.(3-23) by the eigenvector matrix transpose $\boldsymbol{V}^T$ and collecting terms results

$$\boldsymbol{V}^T\left(-\boldsymbol{Q}\Delta\boldsymbol{f}^i - \boldsymbol{Q}\overline{\boldsymbol{f}^i} + \lambda\Delta\boldsymbol{f}^i\right) = \boldsymbol{V}^T\boldsymbol{0}$$

$$-\boldsymbol{V}^T\boldsymbol{V}\boldsymbol{D}\boldsymbol{V}^T\Delta\boldsymbol{f}^i - \boldsymbol{V}^T\boldsymbol{V}\boldsymbol{D}\boldsymbol{V}^T\overline{\boldsymbol{f}^i} + \lambda\boldsymbol{V}^T\Delta\boldsymbol{f}^i = \boldsymbol{0}$$

$$-\boldsymbol{D}\boldsymbol{V}^T\Delta\boldsymbol{f}^i - \boldsymbol{D}\boldsymbol{V}^T\overline{\boldsymbol{f}^i} + \lambda\boldsymbol{V}^T\Delta\boldsymbol{f}^i = \boldsymbol{0} \tag{3-24}$$

Assuming $\boldsymbol{V}^T\Delta\boldsymbol{f}^i = \boldsymbol{x}$ and $\boldsymbol{D}\boldsymbol{V}^T\overline{\boldsymbol{f}^i} = \boldsymbol{b}$, Eq.(3-24) can be converted into

$$-\boldsymbol{D}\boldsymbol{x} + \lambda\boldsymbol{x} = \boldsymbol{b} \tag{3-25}$$

It should be pointed out that by construction the linear transformation $\boldsymbol{x} = \boldsymbol{V}^T\Delta\boldsymbol{f}^i$ preserves the magnitude of the vectors

$$\boldsymbol{x}^T\boldsymbol{x} = \left(\Delta\boldsymbol{f}^i\right)^T\boldsymbol{V}\boldsymbol{V}^T\Delta\boldsymbol{f}^i = \left(\Delta\boldsymbol{f}^i\right)^T\Delta\boldsymbol{f}^i = 1$$

Therefore a system of equations can be constructed

$$\begin{aligned} -\boldsymbol{D}\boldsymbol{x} + \lambda\boldsymbol{x} &= \boldsymbol{b} \\ \boldsymbol{x}^T\boldsymbol{x} &= 1 \end{aligned} \tag{3-26}$$

The Lagrange multiplier λ can be recovered from Eq.(3-26) and the aforementioned KKT systems can be solved.

The solutions to the system described in Eq.(3-26) depends on the right hand vector $\boldsymbol{b}$. The solution method will be discussed for three different cases: 1) with all components of $\boldsymbol{b}$ being non-zeros, 2) when some but not all components of $\boldsymbol{b}$ being zeros and 3) while $\boldsymbol{b}$ being a zero vector. To simply the derivation procedure a two

dimensional problem is considered. The three dimensional problems can be handled in the similar manner.

1) All components of $\boldsymbol{b}$ being non-zeros

The most general case when all the components of $\boldsymbol{b}$ are non-zeros is firstly considered. In this case, as proven by [43], λ must not be an eigenvalue of $\boldsymbol{Q}$. Therefore $(\lambda \boldsymbol{I} - \boldsymbol{D})$ is invertible and $\boldsymbol{x}$ can be expressed as

$$\boldsymbol{x} = (\lambda \boldsymbol{I} - \boldsymbol{D})^{-1} \boldsymbol{b} \tag{3-27}$$

The $\boldsymbol{x}$ term can be eliminated from Eq.(3-27) by inserting Eq.(3-27) into Eq.(3-25) as

$$\boldsymbol{b}^T (\boldsymbol{D} - \lambda \boldsymbol{I})^{-2} \boldsymbol{b} = 1 \tag{3-28}$$

For 2-D structures Eq.(3-28) can be expanded into the component form as

$$\begin{bmatrix} b_1 \\ b_2 \end{bmatrix}^T \begin{bmatrix} \dfrac{1}{(\lambda - \lambda_1)^2} & 0 \\ 0 & \dfrac{1}{(\lambda - \lambda_2)^2} \end{bmatrix} \begin{bmatrix} b_1 \\ b_2 \end{bmatrix} = 1$$

$$\frac{{b_1}^2}{(\lambda - \lambda_1)^2} + \frac{{b_2}^2}{(\lambda - \lambda_2)^2} = 1 \tag{3-29}$$

As shown in [44] the above system yields at most four distinct real roots for the Lagrange multiplier λ, with one root larger than λ_1, two roots between λ_1 and λ_2, and one root smaller than λ_2. However as stated before the 2nd order condition Eq.(3-21) filtered out all the solutions except for the root greater than λ_1, and this root can be found through iterative methods with a starting point in the section of $[\lambda_1, \lambda_1 + \|b_1\|]$. Letting the solution

of the Eq.(3-29) λ^*, the optimizer $\Delta \boldsymbol{f}^{i*}$ of the problem in Eq.(3-15) can be found from Eq.(3-23), as

$$\Delta \boldsymbol{f}^{i*} = \left(\lambda^* \boldsymbol{I} - \boldsymbol{Q}\right)^{-1} \boldsymbol{Q}\,\overline{\boldsymbol{f}^i}$$

Finally the global optimum solution can be evaluated as

$$U_{\max} = \left[\left(\overline{\boldsymbol{f}^i} + \Delta \boldsymbol{f}^i\right)^T \boldsymbol{Q}\left(\overline{\boldsymbol{f}^i} + \Delta \boldsymbol{f}^i\right)\right]_{\max} = \left(\Delta \boldsymbol{f}^{i*}\right)^T \boldsymbol{Q}\Delta \boldsymbol{f}^{i*} + 2\left(\Delta \boldsymbol{f}^{i*}\right)^T \boldsymbol{Q}\,\overline{\boldsymbol{f}^i} + \left(\overline{\boldsymbol{f}^i}\right)^T \boldsymbol{Q}\,\overline{\boldsymbol{f}^i} \qquad (3\text{-}30)$$

Thus the objective function value of the problem in Eq.(3-14) is calculated.

In order to solve the design problem using a gradient based method, the sensitivity of the objective function is required. The sensitivity analysis starts with differentiating the solution found as in Eq. (3-30) with respect to the design variable a_k

$$\begin{aligned} \frac{dU_{\max}}{da_k} &= \frac{d\left[\left(\overline{\boldsymbol{f}^i} + \Delta \boldsymbol{f}^i\right)^T \boldsymbol{Q}\left(\overline{\boldsymbol{f}^i} + \Delta \boldsymbol{f}^i\right)\right]}{da_k} \\ &= \left(\overline{\boldsymbol{f}^i} + \Delta \boldsymbol{f}^i\right)^T \frac{d\boldsymbol{Q}}{da_k}\left(\overline{\boldsymbol{f}^i} + \Delta \boldsymbol{f}^{i*}\right) + 2\left(\overline{\boldsymbol{f}^i} + \Delta \boldsymbol{f}^i\right)^T \boldsymbol{Q}\frac{d\Delta \boldsymbol{f}^i}{da_k} \end{aligned} \qquad (3\text{-}31)$$

Terms $d\boldsymbol{Q}/da_k$ and $d\Delta \boldsymbol{f}^i/da_k$ require evaluations. The derivation of the $d\boldsymbol{Q}/da_k$ term is straight forward since $\boldsymbol{Q} = \boldsymbol{A}^T \boldsymbol{K}\boldsymbol{A}$ by construction. Thus

$$\frac{d\boldsymbol{Q}}{da_k} = \boldsymbol{A}^T \frac{d\boldsymbol{K}}{da_k}\boldsymbol{A} \qquad (3\text{-}32)$$

where the calculation for $d\boldsymbol{K}/da_k$ is well known and can be found in [35].

Moving on to the $d\Delta \boldsymbol{f}^i/da_k$ term, the analysis starts with differentiating both sides of the stationarity condition in Eq.(3-23) as

$$\frac{d\left(\boldsymbol{Q}\Delta \boldsymbol{f}^i\right)}{da_k} + \frac{d\left(\boldsymbol{Q}\,\overline{\boldsymbol{f}^i}\right)}{da_k} = \frac{d\left(\lambda \Delta \boldsymbol{f}^i\right)}{da_k} \qquad (3\text{-}33)$$

Expanding Eq.(3-33) and collecting terms yields

$$\frac{d\boldsymbol{Q}}{da_k}\Delta\boldsymbol{f}^i + \boldsymbol{Q}\frac{d\Delta\boldsymbol{f}^i}{da_k} + \frac{d\boldsymbol{Q}}{da_k}\overline{\boldsymbol{f}^i} = \lambda\frac{d\Delta\boldsymbol{f}^i}{da_k} + \frac{d\lambda}{da_k}\Delta\boldsymbol{f}^i$$

The term $d\Delta\boldsymbol{f}^i/da_k$ can be expressed as a function of $d\boldsymbol{Q}/da_k$ and $d\lambda/da_k$, as shown in Eq.(3-34)

$$\frac{d\Delta\boldsymbol{f}^i}{da_k} = \left(\lambda\boldsymbol{I}-\boldsymbol{Q}\right)^{-1}\frac{d\boldsymbol{Q}}{da_k}\left(\overline{\boldsymbol{f}^i}+\Delta\boldsymbol{f}^i\right) - \frac{d\lambda}{da_k}\left(\lambda\boldsymbol{I}-\boldsymbol{Q}\right)^{-1}\Delta\boldsymbol{f}^i \tag{3-34}$$

The $d\boldsymbol{Q}/da_k$ is already known and $d\lambda/da_k$ can be evaluated through introducing the $\left(\Delta\boldsymbol{f}^i\right)^T\Delta\boldsymbol{f}^i - 1 = 0$ relation shown in Eq.(3-22). Differentiating both sides of Eq.(3-22) yields

$$\left(\Delta\boldsymbol{f}^i\right)^T\frac{d\Delta\boldsymbol{f}^i}{da_k} + \frac{d\left(\Delta\boldsymbol{f}^i\right)^T}{da_k}\Delta\boldsymbol{f}^i = 2\left(\Delta\boldsymbol{f}^i\right)^T\frac{d\Delta\boldsymbol{f}^i}{da_k} = 0 \tag{3-35}$$

Re-expressing the stationarity condition in Eq.(3-23) as $\Delta\boldsymbol{f}^i = \left(\lambda\boldsymbol{I}-\boldsymbol{Q}\right)^{-1}\boldsymbol{Q}\overline{\boldsymbol{f}^i}$ and plugging into Eq.(3-35) result in

$$\left(\Delta\boldsymbol{f}^i\right)^T\left[\frac{d\left(\lambda\boldsymbol{I}-\boldsymbol{Q}\right)^{-1}}{da_k}\boldsymbol{Q}\overline{\boldsymbol{f}^i} + \left(\lambda\boldsymbol{I}-\boldsymbol{Q}\right)^{-1}\frac{d\boldsymbol{Q}}{da_k}\overline{\boldsymbol{f}^i}\right] = 0 \tag{3-36}$$

Following the chain rule Eq.(3-36) can be rewritten as

$$\frac{d\lambda}{da_k} = \frac{\left(\Delta\boldsymbol{f}^i\right)^T\left(\lambda\boldsymbol{I}-\boldsymbol{Q}\right)^{-1}\dfrac{d\boldsymbol{Q}}{da_k}\left(\Delta\boldsymbol{f}^i+\overline{\boldsymbol{f}^i}\right)}{\left(\Delta\boldsymbol{f}^i\right)^T\left(\lambda\boldsymbol{I}-\boldsymbol{Q}\right)^{-1}\Delta\boldsymbol{f}^i} \tag{3-37}$$

Thus $d\lambda/da_k$ is expressed in terms of $d\boldsymbol{Q}/da_k$, which is derived previously. By inserting this result into Eq.(3-34), $d\Delta\boldsymbol{f}^i/da_k$ can also be considered as a function of $d\boldsymbol{Q}/da_k$ and the sensitivity $dU_{\max}/da_k$, as shown in Eq.(3-31), can be evaluated. These results complete the analysis when all the components of $\boldsymbol{b}$ are non-zeros.

2) Some but not all components of $\boldsymbol{b}$ being zeros

For the second case, it is assumed that some but not all of the components of vector $\boldsymbol{b}$ are zeros. The physical meaning of this is that the nominal load has the same directions as the eigenvectors of the $\boldsymbol{Q}$ matrix. For the two dimensional case the system described in Eq.(3-26) can be rewritten into the component form as

$$\begin{gathered} -\begin{bmatrix} \lambda_1 & 0 \\ 0 & \lambda_2 \end{bmatrix}\begin{bmatrix} x_1 \\ x_2 \end{bmatrix} + \lambda \begin{bmatrix} x_1 \\ x_2 \end{bmatrix} = \begin{bmatrix} b_1 \\ b_2 \end{bmatrix} \\ \begin{bmatrix} x_1 \\ x_2 \end{bmatrix}^T \begin{bmatrix} x_1 \\ x_2 \end{bmatrix} = x_1^2 + x_2^2 = 1 \end{gathered} \tag{3-38}$$

The assumption on the vector $\boldsymbol{b}$ implies that either b_1 or b_2 equals to zero. Therefore the system can be further broken down into two circumstances: when $b_1 = 0$ and when $b_2 = 0$, with the supposition that $\lambda_1 > \lambda_2$. By using $\boldsymbol{v}_1$ and $\boldsymbol{v}_2$ to indicate the eigenvectors associated with the eigenvalues, the case when $b_1 = 0$ represents when $\overline{\boldsymbol{f}^i}$ is aligned with $\boldsymbol{v}_2$ while $b_2 = 0$ implies that $\overline{\boldsymbol{f}^i}$ is in the direction of $\boldsymbol{v}_1$.

In case of $b_1 = 0$, Eq.(3-38) can be written as a set of algebraic equations:

$$\begin{gathered} (\lambda - \lambda_1) x_1 = 0 \\ (\lambda - \lambda_2) x_2 = b_2 \\ x_1^2 + x_2^2 = 1 \end{gathered}$$

Working from the relation $(\lambda - \lambda_1) x_1 = 0$, it requires either $x_1 = 0$ or $\lambda - \lambda_1 = 0$. If $x_1 = 0$, from the condition $x_1^2 + x_2^2 = 1$, x_2 can be solved as $x_2 = \pm 1$, $\lambda = b_2 / x_2 + \lambda_2$, or $\lambda = \lambda_2 \pm |b_2|$. On the other hand if $\lambda - \lambda_1 = 0$, it implies that $\lambda = \lambda_1$, $x_2 = b_2 / (\lambda_1 - \lambda_2)$. It should be noted that the condition $x_1^2 + x_2^2 = 1$ requires $|x_2| \le 1$. Consequently $|x_2| = |b_2 / (\lambda_1 - \lambda_2)| = |b_2| / (\lambda_1 - \lambda_2) \le 1$ (since $\lambda_1 > \lambda_2$), therefore in order for a solution to exist the following relation must hold:

$\lambda_1 \geq \lambda_2 + |b_2|$. Furthermore the 2nd order condition implies that $\lambda \geq \lambda_1 > \lambda_2$. Therefore combining all the above analyses an conclusion could be reached that when $\lambda_1 < \lambda_2 + |b_2|$, $\lambda = \lambda_2 + |b_2|$ with $x_1 = 0$, $x_2 = b_2/|b_2|$; and when $\lambda_1 \geq \lambda_2 + |b_2|$, $\lambda = \lambda_1$ with $x_2 = b_2/(\lambda_1 - \lambda_2)$ and $x_1 = \pm\sqrt{1-\left[b_2/(\lambda_1 - \lambda_2)\right]^2}$.

Now considering the other case when $b_2 = 0$, a similar set of algebraic equations can be constructed as

$$(\lambda - \lambda_1)x_1 = b_1$$
$$(\lambda - \lambda_2)x_2 = 0$$
$$x_1^2 + x_2^2 = 1$$

Following the same idea the relation $(\lambda - \lambda_2)x_2 = 0$ requires either $x_2 = 0$ or $\lambda - \lambda_2 = 0$. When $x_2 = 0$, x_1 can be solved as $x_1 = \pm 1$, and $\lambda = b_1/x_1 + \lambda_1$, or $\lambda = \lambda_1 \pm |b_1|$. When $\lambda - \lambda_2 = 0$, $\lambda = \lambda_2$ and $x_1 = b_1/(\lambda_2 - \lambda_1)$. However the relation $x_1^2 + x_2^2 = 1$ confines the magnitude of the x_1 term to be $|x_1| \leq 1$, which can be extended to $|x_1| = |b_1/(\lambda_1 - \lambda_2)| = |b_1|/(\lambda_1 - \lambda_2) \leq 1$, or $\lambda = \lambda_2 \leq \lambda_1 - |b_2|$, and it violates the 2nd order condition which necessitates that $\lambda \geq \lambda_1 > \lambda_2$. Therefore $\lambda - \lambda_2 = 0$ is not a valid solution and the only solution to this problem is $\lambda = \lambda_1 + |b_1|$, with $x_1 = b_1/|b_1|$.

The above discussion provides the completes description of the derivation for the case when some but not all of $\boldsymbol{b}$'s components equal to zeros. Once the correct solution for the Lagrange multiplier λ is identified one can proceed to the sensitivity analysis, which is identical to the previous non-zeros case and will not be repeated here.

3) The vector $\boldsymbol{b}$ being a zero vector

In the third case, $\boldsymbol{b}$ is assumed to be a zero vector. The physical meaning of this special case is that the nominal load $\overline{\boldsymbol{f}^i} = \boldsymbol{0}$, as shown in Figure 3-8:

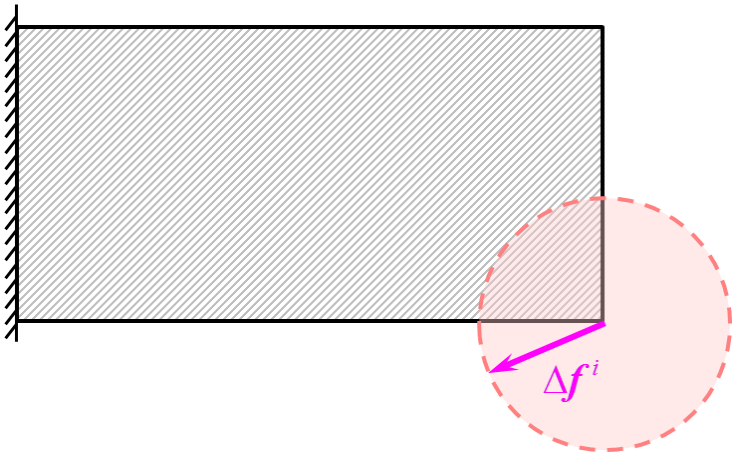

Figure 3-8 The $\overline{\boldsymbol{f}^i} = \boldsymbol{0}$ Situation

It can be proven by definition $\boldsymbol{D}\boldsymbol{V}^T \overline{\boldsymbol{f}^i} = \boldsymbol{b}$. Since both $\boldsymbol{D}$ and $\boldsymbol{V}^T$ are full rank, the only solution for $\boldsymbol{b} = \boldsymbol{0}$ is $\overline{\boldsymbol{f}^i} = \boldsymbol{0}$.

With the absence of the nominal load, the lower problem can be expressed as

$$\begin{aligned} \max \quad & \left(\Delta \boldsymbol{f}^i\right)^T \boldsymbol{Q} \Delta \boldsymbol{f}^i \\ \text{s.t.} \quad & \left(\Delta \boldsymbol{f}^i\right)^T \Delta \boldsymbol{f}^i \le 1 \end{aligned} \tag{3-39}$$

The 1st order KKT conditions can be found as

$$\frac{dL}{d\Delta \boldsymbol{f}^i} = -2\boldsymbol{Q}\Delta \boldsymbol{f}^i + 2\lambda \Delta \boldsymbol{f}^i = \boldsymbol{0} \tag{3-40}$$

$$\left(\Delta \boldsymbol{f}^i\right)^T \Delta \boldsymbol{f}^i - 1 \le 0 \tag{3-41}$$

$$\lambda \ge 0 \tag{3-42}$$

$$\lambda \left[\left(\Delta \boldsymbol{f}^i\right)^T \Delta \boldsymbol{f}^i - 1 \right] = 0 \tag{3-43}$$

As pointed out before, from the dual feasibility condition in Eq.(3-42) and the complementary slackness condition in (3-43) it can be seen that the constraint $\left(\Delta \boldsymbol{f}^i\right)^T \Delta \boldsymbol{f}^i \le 1$ must be active at the optimum, therefore the primal feasibility condition in Eq.(3-41) can be converted into an equality constraint. Combining the Eq.(3-40) and Eq.(3-41) an eigenvalue problem can be defined and solving this problem yields the optimum candidates. Furthermore by employing the 2nd order condition, which has the same expression as Eq.(3-21), the global optima can be filtered out from the candidate pool, since only the greatest eigenvalue of the $\boldsymbol{Q}$ matrix satisfies the 2nd order condition. Thus the solution to the Eq.(3-39) problem can be found as

$$\begin{aligned} U_{\max} &= \left[\left(\Delta \boldsymbol{f}^i\right)^T \boldsymbol{Q} \Delta \boldsymbol{f}^i \right]_{\max} \\ &= \left(\Delta \boldsymbol{f}^{i*}\right)^T \boldsymbol{Q} \Delta \boldsymbol{f}^{i*} \\ &= \lambda^* \end{aligned} \tag{3-44}$$

where λ^* is the greatest eigenvalue of $\boldsymbol{Q}$ and $\Delta \boldsymbol{f}^{i*}$ is the corresponding eigenvector. The sensitivity analysis of the solution found in Eq.(3-44) follows the eigenvalue differentiation.

$$\frac{d\lambda^*}{da_k} = \left(\Delta \boldsymbol{f}^{i*}\right)^T \frac{d\boldsymbol{Q}}{da_k} \Delta \boldsymbol{f}^{i*}$$

The calculation of $d\boldsymbol{Q}/da_k$ is the same as in Eq.(3-32) and it completes the sensitivity analysis.

With the function value of the lower level problem evaluated and the sensitivity analysis completed, the upper level design problem, as formulated in Eq.(3-14), is ready to be solved by standard gradient based topology optimization algorithms, such as the

Sorting Method, Optimization Criteria (OC) or Method of Moving Asymptotes (MMA) [35].

3.4 Numerical Example

In this section, a design problem of a cantilever under load uncertainty is discussed to demonstrate the effectiveness of the convex modeling based topology optimization method.

In this example a rectangular design domain with left edge fixed is considered, as shown in Figure 3-9 (a). The structure is subject to an unknown-but-bounded load with uncertainty applied at the lower right corner. The design objective is to obtain higher overall stiffness hence the strain energy of the structure is minimized. The problem is solved using the convex modeling based min compliance formulation.

To serve the purpose of comparison the problem is also solved with a traditional method through replacing the load with uncertainty by deterministic loads. Two comparisons are made, first with a single static load and second with a multiple-load-case with loads pointing to different directions, as shown in Figure 3-9 (b) and Figure 3-9 (c) respectively. The applied loads are indicated by the arrows.

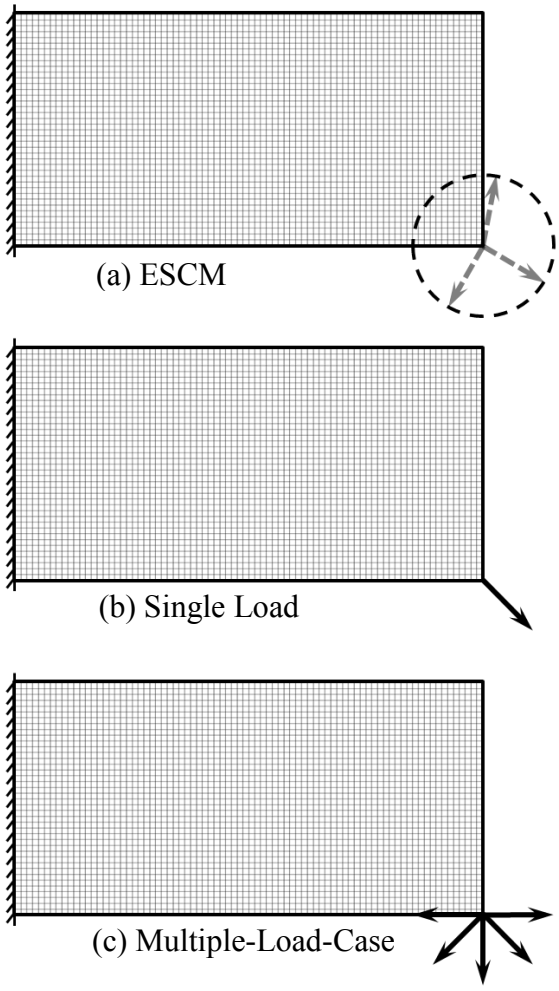

Figure 3-9 Design Domain and Boundary Conditions of the Cantilever

The optimum structures generated for the three problems are illustrated in Figure 3-10. The arrows indicate the directions of the loads which yield the maximum strain energies for the configurations, namely the worst loads.

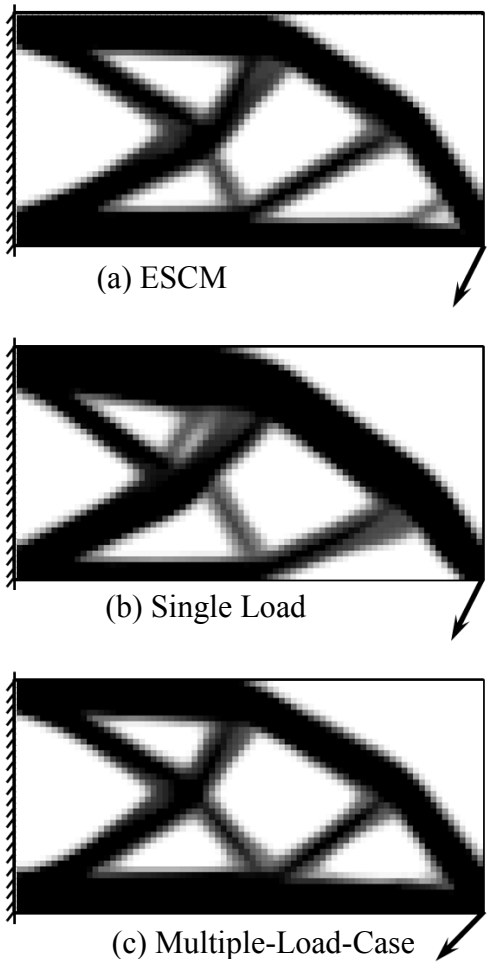

Figure 3-10 Results of Cantilever Example

It is observed from this example that the convex modeling based method and the multiple-load-case example have yielded similar configurations. The reason is that during each iteration of the convex modeling based design process, the worst case scenario, or the worst load, of the current configuration was used; similarly for the multiple-load-case situation, multiple loads pointing to different directions were considered simultaneously. Since the worst load was covered by the region spanned by the multiple load cases, the result obtained is similar to that of the convex modeling based method. The effect of the worst load is considered at the cost of computational complexity in the multiple load case

strategy. For the single deterministic load scenario, in contrast, only one direction was considered while other possibilities were ignored. Consequently this resulted in poor performance under the worst load, as seen in Table 3-1, where the maximum strain energies of the optimized structures for the three different situations are listed.

Table 3-1 Strain Energy under the Worst Load

	Convex Model	Single	Multiple
Strain Energy	83.90	190.16	84.46

The difference between the convex modeling based and the multiple-load-case is that in the first method the worst load, which is automatically determined, was always used. While for the later one all the applied excitations are considered equally. Only with a sufficiently large number of loads the method based on multiple load cases yields a similar result as the convex modeling based method. It is also worth noting that compared to the convex modeling based method, the computational cost of the multiple-load-case method is much higher, since numerous analyses must be performed. In this example five load cases are considered, which implies that within every iteration of the optimization algorithm, five FEM analyses are required, compared to two FEM analyses of the convex modeling based method.

Through this example the effectiveness of the convex modeling based method in solving topology optimization problem is demonstrated. It can be seen that the convex

modeling based method extends the capacity of the topology optimization when load uncertainties are involved.

Chapter 4

Protective Structure Design

4.1 Introduction to Protective Structure Design

The protective structure design problem has a wide range of engineering applications. For example in packaging design, one of the primary objectives is to protect its content when a package is dropped. Figure 4-1 illustrates a typical packaging drop test.

Figure 4-1 Packaging Drop Test [5]

However the protective structure design problem can be very complicated. Considering the drop test illustrated above, several challenges can be identified: the direction of the

[5] Resource: http://www.opti-pack.org/10700.2

impact force when the package hits the floor is uncertain; both the packaging and its content needs to be considered; and during free fall the package is unconstrained. In this chapter, a protective structure design problem is investigated due to its wide range of engineering application and high level of complexity.

Consider the problem shown in Figure 4-2:

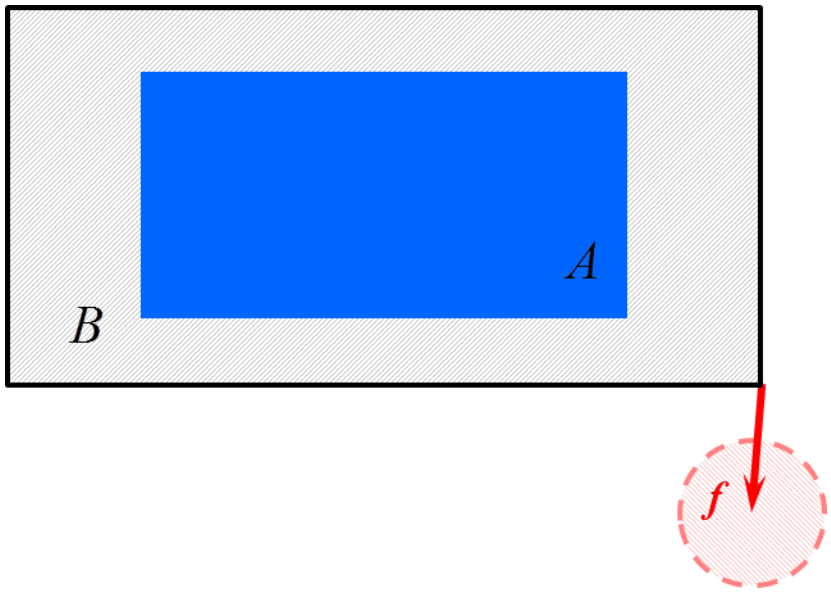

Figure 4-2 Protective Structure Design under Load Uncertainty

The design domain is unconstrained and is composed of two regions: the inner region *A* and the outer region *B*; region *A* is non-designable and needs to be protected. The design target is to find the optimum layout in region *B* which provides the maximum protection to region *A* under an uncertain impact at the lower right corner.

There are several challenges worth pointing out in solving this problem: Firstly the external load is uncertain and consequently deterministic based topology optimization method cannot be used. Secondly there are multiple objectives for the design: protecting

region *A* while maintaining the overall structure integrity. The protection requires minimum amount of strain energy in the *A* region and the structural integrity consideration prefers a lower total strain energy. Therefore it is a multi-objective optimization problem. Thirdly the structure is unconstrained. A large rigid body motion will be involved when external load is applied and the response of the structure can no longer be analyzed by a static method.

In order to solve this protective structural design problem, the convex modeling based topology optimization method is combined with the regional strain energy formulation and the inertial relief method.

4.1.1 Regional Strain Energy Formulation

Strain energy of the whole design domain is used as the objective function in most topology optimization formulations, where an optimum structure which yields the maximum overall rigidity can be achieved by minimizing the total strain energy. A regional strain energy formulation was proposed by Gea [45] for solving energy absorbing compliant structure design problems. In this method the strain energy of a specified region in the design domain is considered. Combining with the total strain energy, the rigidity and compliance of the structure can be obtained simultaneously. Consider the problem shown in Figure 4-3 for example:

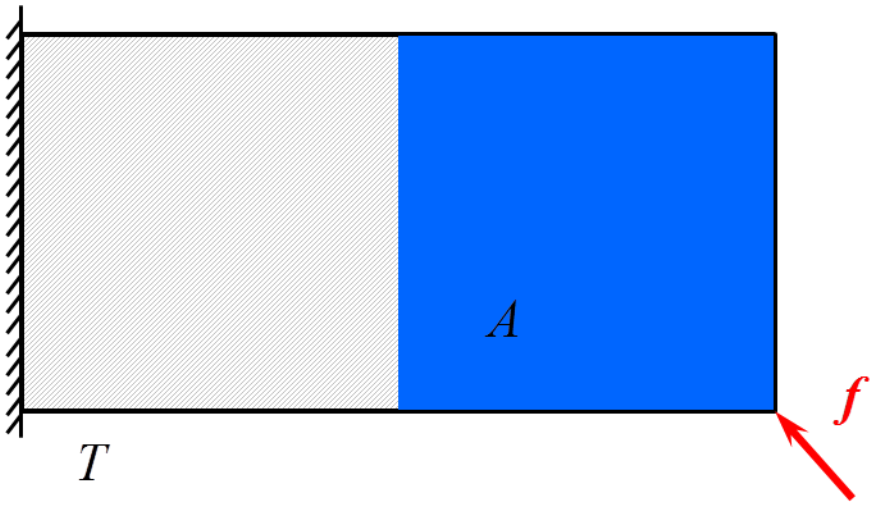

Figure 4-3 Regional Strain Energy Formulation

Region *A* is a portion of the total design domain and it should absorb as much strain energy as possible to protect the other part of the structure; at the same time the overall structural integrity must be maintained. To achieve both goals Eq.(4-1) is used as the new objective function

$$\min \quad \frac{U_T}{U_A} \tag{4-1}$$

Clearly both requirements can be satisfied since minimizing U_T keeps the structural integrity while minimizing $1/U_A$ is equivalent to maximizing U_A (U_A is the strain energy and $U_A \geq 0$).

For discretized system the regional strain energy U_A can be calculated through summing the element strain energy of the elements in region *A*:

$$U_A = \sum_i \boldsymbol{u}_e^T \boldsymbol{K}_e \boldsymbol{u}_e \ , \ i \in A \tag{4-2}$$

Denoting the part of the global stiffness matrix associated with region *A* assembled from Eq.(4-2) as $\boldsymbol{K}_A$, the relation can also be written as

$$U_A = \boldsymbol{u}^T \boldsymbol{K}_A \boldsymbol{u} \tag{4-3}$$

4.1.2 Inertial Relief Method

Traditionally the majority of topology optimization problems focus on solving static problems. However in many practical problems dynamic physics are involved. For example in the aforementioned packaging drop test problem the system cannot be considered as static during the impact since the packaging is unconstrained and both rigid body displacement and elastic deformation are involved. Compared to the static analysis, the dynamic analysis requires a much higher computational effort. Furthermore the sensitivity information which is essential for the topology optimization cannot be easily obtained, since the solution to the dynamic problem is calculated at each time step [46]. The inertial relief method, which considers the dynamic effect but has a complexity level of static problems, can be utilized in solving dynamic topology optimization problems.

The inertial relief method approximates the dynamic solution to unconstrained systems under constant or slowly varying load problems [47] and accurate results can be obtained when the frequency of the external load is much lower than the structure's first natural frequency [48]. As summarized by Song et al. [49], when a time independent load is applied to an unconstrained structure the dynamic equilibrium equation can be written as

$$\boldsymbol{K}\boldsymbol{u}_{Total} + \boldsymbol{M}\ddot{\boldsymbol{u}}_{Total} = \boldsymbol{f} \tag{4-4}$$

where $\boldsymbol{M}$ is the global mass matrix and the second time derivative of the displacement $\ddot{\boldsymbol{u}}$ is the acceleration. The subscript *Total* indicates total value and it can be decoupled into

the rigid body motion part (denoted by the subscript *Rigid*) and elastic deformation part, as in Eq.(4-5) and Eq.(4-6)

$$\boldsymbol{u}_{Total} = \boldsymbol{u}_{Rigid} + \boldsymbol{u} \tag{4-5}$$

$$\ddot{\boldsymbol{u}}_{Total} = \ddot{\boldsymbol{u}}_{Rigid} + \ddot{\boldsymbol{u}} \tag{4-6}$$

By inserting these relations into Eq.(4-4) the governing equation becomes

$$\boldsymbol{K}\boldsymbol{u}_{Rigid} + \boldsymbol{K}\boldsymbol{u} + \boldsymbol{M}\ddot{\boldsymbol{u}}_{Rigid} + \boldsymbol{M}\ddot{\boldsymbol{u}} = \boldsymbol{f} \tag{4-7}$$

Since the rigid body motion will not generate any internal force within the structure, $\boldsymbol{K}\boldsymbol{u}_{Rigid} = \boldsymbol{0}$ and therefore can be removed from Eq.(4-7). Furthermore based on the unconstrained structure subject to time independent load assumption, the acceleration due to elastic deformation is negligible compared to rigid body acceleration. Hence $\boldsymbol{M}\ddot{\boldsymbol{u}}$ can also be neglected and Eq.(4-7) can be simplified to

$$\boldsymbol{K}\boldsymbol{u} + \boldsymbol{M}\ddot{\boldsymbol{u}}_{Rigid} = \boldsymbol{f} \tag{4-8}$$

The term $\boldsymbol{M}\ddot{\boldsymbol{u}}_{Rigid}$ represents the inertial force generated by the rigid body motion and Eq.(4-8) is the governing equation used in the inertial relief method.

It is worth pointing out that moving the inertial force term to the right side of Eq.(4-8) yields

$$\boldsymbol{K}\boldsymbol{u} = \boldsymbol{f} - \boldsymbol{M}\ddot{\boldsymbol{u}}_{Rigid} \tag{4-9}$$

The right hand side terms can be considered as the new load and thus the original dynamic problem is converted into a static problem.

In Eq.(4-9) the rigid body acceleration $\ddot{\boldsymbol{u}}_{Rigid}$ can be found from rigid body dynamics. The motion at any point of a rigid body can be expressed by the motion of a given reference

point [50]. Therefore when choosing the center of gravity (CG) as the reference point, the motion at any node of a meshed geometry can be described by the motion of its CG, as shown in Figure 4-4

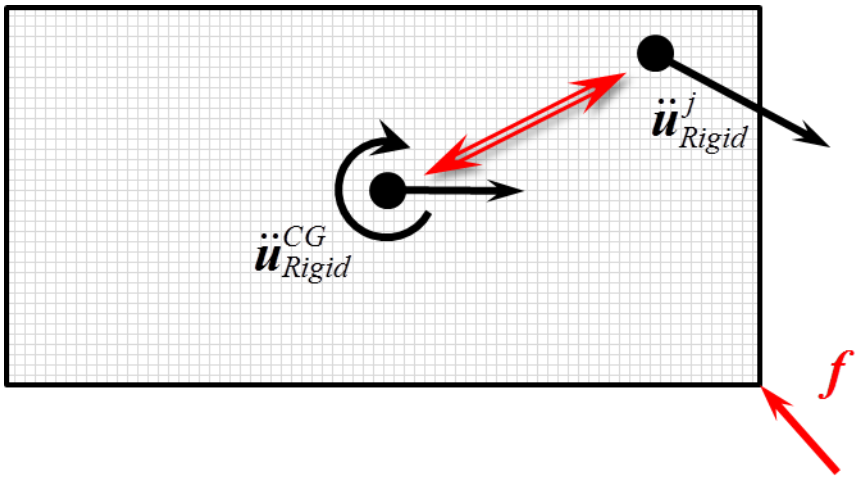

Figure 4-4 Rigid Body Motion of Meshed Geometry

The acceleration of j^{th} node $\ddot{\boldsymbol{u}}^{j}_{Rigid}$ can be calculated from the CG acceleration $\ddot{\boldsymbol{u}}^{CG}_{Rigid}$ and a geometric rigid body transformation matrix $\boldsymbol{R}^{j}$

$$\ddot{\boldsymbol{u}}^{j}_{Rigid} = \boldsymbol{R}^{j}\ddot{\boldsymbol{u}}^{CG}_{Rigid}$$

where

$$\ddot{\boldsymbol{u}}^{j}_{Rigid} = \begin{bmatrix} \ddot{u}^{j}_{x} \\ \ddot{u}^{j}_{y} \end{bmatrix}, \boldsymbol{R}^{j} = \begin{bmatrix} 1 & 0 & -(y_j - y_{CG}) \\ 0 & 1 & (x_j - x_{CG}) \end{bmatrix}, \ddot{\boldsymbol{u}}^{CG}_{Rigid} = \begin{bmatrix} \ddot{u}^{CG}_{x} \\ \ddot{u}^{CG}_{y} \\ \ddot{\theta}^{CG}_{z} \end{bmatrix}$$

The coordinates of the CG x_{CG} and y_{CG} can be calculated as

$$\begin{bmatrix} x_{CG} \\ y_{CG} \end{bmatrix} = \frac{1}{\sum_{i=1}^{n} m_i} \sum_{i=1}^{n} \left(m_i \begin{bmatrix} x_i \\ y_i \end{bmatrix} \right) \tag{4-10}$$

where x_i, y_i and m_i are the coordinates and the mass for the i^{th} node respectively.

The global acceleration vector $\ddot{\boldsymbol{u}}_{Rigid}$ can be obtained through assembling the nodal vectors, which yields

$$\ddot{\boldsymbol{u}}_{Rigid} = \boldsymbol{R}\ddot{\boldsymbol{u}}_{Rigid}^{CG}$$

where

$$\ddot{\boldsymbol{u}}_{Rigid} = \begin{bmatrix} \left[\ddot{\boldsymbol{u}}_{Rigid}^{1}\right] \\ \left[\ddot{\boldsymbol{u}}_{Rigid}^{2}\right] \\ \vdots \\ \left[\ddot{\boldsymbol{u}}_{Rigid}^{n}\right] \end{bmatrix}, \boldsymbol{R} = \begin{bmatrix} \left[\boldsymbol{R}^{1}\right] \\ \left[\boldsymbol{R}^{2}\right] \\ \vdots \\ \left[\boldsymbol{R}^{n}\right] \end{bmatrix}$$

The resultant load acting on the CG can also be obtained from the same transformation:

$$\boldsymbol{f}^{CG} = \boldsymbol{R}^{T}\boldsymbol{f}$$

The concept of inertial relief requires that the resultant load on the CG $\boldsymbol{f}^{CG}$ must be balanced by the inertial force about the CG, as described in Eq.(4-11).

$$\boldsymbol{R}^{T}\boldsymbol{M}\boldsymbol{R}\ddot{\boldsymbol{u}}_{Rigid}^{CG} = \boldsymbol{f}^{CG} = \boldsymbol{R}^{T}\boldsymbol{f} \tag{4-11}$$

It should be pointed out that the elastic deformation $\boldsymbol{u}$ is orthogonal to the rigid body shapes $\boldsymbol{\varphi}_i$. This can be proven through mode analysis. The rigid body shapes $\boldsymbol{\varphi}_i$ are eigenvectors corresponding to the eigenvalues $\lambda_i = 0$, while the elastic deformation $\boldsymbol{u}$ can be expressed as a linear combination of other eigenvectors corresponding to the non-zero eigenvalues, as shown in Eq.(4-12)

$$\boldsymbol{\varphi}_i^{T}\boldsymbol{M}\boldsymbol{u} = 0 \tag{4-12}$$

Since the rows of the geometric rigid body transformation matrix $\boldsymbol{R}$ can be considered as linear combinations of the rigid body shapes $\boldsymbol{\varphi}_i$, Eq.(4-12) can be extended into

$$\boldsymbol{R}^{T}\boldsymbol{M}\boldsymbol{u} = \boldsymbol{0} \tag{4-13}$$

Combining the governing equation in Eq.(4-8) with Eq.(4-11) and Eq.(4-13) yields

$$\begin{bmatrix} \boldsymbol{K} & \boldsymbol{MR} \\ \boldsymbol{R}^T\boldsymbol{M} & \boldsymbol{R}^T\boldsymbol{MR} \end{bmatrix} \begin{bmatrix} \boldsymbol{u} \\ \ddot{\boldsymbol{u}}_{Rigid}^{CG} \end{bmatrix} = \begin{bmatrix} \boldsymbol{f} \\ \boldsymbol{R}^T\boldsymbol{f} \end{bmatrix} \tag{4-14}$$

Solving Eq.(4-14) gives the elastic deformation $\boldsymbol{u}$ and the CG acceleration $\ddot{\boldsymbol{u}}_{Rigid}^{CG}$ simultaneously. The unconstrained problem is therefore solved by the inertial relief method.

4.2 Problem Formulation

For a typical protective structural design problem as illustrated in Figure 4-2, the design requires that strain energy absorbed by region *A*, denoted by U_A, is minimized and protected. Meanwhile the strain energy of the whole structure U_T also needs to be minimized to maintain the overall structure integrity. By utilizing the concept of the regional strain energy method introduced in section 4.1.1, the objective function can be defined as

$$\min_{\boldsymbol{a}} \quad U_A U_T \tag{4-15}$$

It should be noted that since this is a multi-objective optimization problem, and therefore when converting the multiple objectives to a single objective the choice may not be unique. For the problem in Figure 4-2 for example, the weighted sum formulation can also be used, as in Eq.(4-16)

$$\min_{\boldsymbol{a}} \quad w_A U_A + w_T U_T \tag{4-16}$$

However specifying the weightings w_A and w_T might be problematic. The multiplication formulation shown in Eq.(4-15) is used as the objective function for its simplicity.

In this problem external loads have uncertainties. The convex modeling based topology optimization method can be used to solve the uncertainty problem. The worst structure response can be identified using the convex modeling based method under a given load uncertainty and this worst case, indicated by $(U_A)_{\max}$, can be used as the new design objective. The convex modeling based method also gives the load that yields the worst response, namely the worst load $\boldsymbol{f}^*$. The total strain energy can be evaluated using $\boldsymbol{f}^*$, and the design problem with load uncertainty can be formulated as

$$\begin{aligned} \min_{\boldsymbol{a}} \quad & (U_A)_{\max}\left[U_T(\boldsymbol{f})\right] \\ \text{s.t.} \quad & V \le V_0 \\ & \boldsymbol{K}\boldsymbol{u} = \boldsymbol{f} \\ & \boldsymbol{f} = \boldsymbol{A}\boldsymbol{f}^i \\ & \boldsymbol{f}^i = \overline{\boldsymbol{f}^i} + \Delta\boldsymbol{f}^i \\ & (\Delta\boldsymbol{f})^T \Delta\boldsymbol{f} \le 1 \end{aligned} \tag{4-17}$$

The structure in Figure 4-2 is unconstrained during the impact. In this case static analysis $\boldsymbol{K}\boldsymbol{u} = \boldsymbol{f}$ can no longer be used. This issue can be resolved by implementing the inertial relief method explained in section 4.1.2. Consider the inertial relief equation in Eq.(4-14):

$$\begin{bmatrix} \boldsymbol{K} & \boldsymbol{M}\boldsymbol{R} \\ \boldsymbol{R}^T\boldsymbol{M} & \boldsymbol{R}^T\boldsymbol{M}\boldsymbol{R} \end{bmatrix} \begin{bmatrix} \boldsymbol{u} \\ \ddot{\boldsymbol{u}}_{Rigid}^{CG} \end{bmatrix} = \begin{bmatrix} \boldsymbol{f} \\ \boldsymbol{R}^T\boldsymbol{f} \end{bmatrix}$$

It can be simplified into

$$\hat{\boldsymbol{K}}\hat{\boldsymbol{u}} = \boldsymbol{G}\boldsymbol{f} \tag{4-18}$$

where

$$\hat{\boldsymbol{K}} = \begin{bmatrix} \boldsymbol{K} & \boldsymbol{M}\boldsymbol{R} \\ \boldsymbol{R}^T\boldsymbol{M} & \boldsymbol{R}^T\boldsymbol{M}\boldsymbol{R} \end{bmatrix},\ \hat{\boldsymbol{u}} = \begin{bmatrix} \boldsymbol{u} \\ \ddot{\boldsymbol{u}}_{Rigid}^{CG} \end{bmatrix},\ \boldsymbol{G} = \begin{bmatrix} \boldsymbol{I} \\ \boldsymbol{R}^T \end{bmatrix}$$

By defining a rectangular matrix

$$\boldsymbol{L} = \left[\boldsymbol{I}_{nxn} \quad \boldsymbol{0}\right]$$

The displacement $\boldsymbol{u}$ can be extracted from $\hat{\boldsymbol{u}}$ as $\boldsymbol{u} = \boldsymbol{L}\hat{\boldsymbol{u}}$, and it can be calculated using Eq.(4-18), as

$$\boldsymbol{u} = \boldsymbol{L}\hat{\boldsymbol{K}}^{-1}\boldsymbol{G}\boldsymbol{f} \tag{4-19}$$

Replacing the original governing equation with the modified inertial relief governing equation in Eq.(4-19), the design problem can be defined as

$$\begin{aligned} \min_{\boldsymbol{a}} \quad & \left(U_A\right)_{\max}\left[U_T\left(\boldsymbol{f}\right)\right] \\ \text{s.t.} \quad & V \le V_0 \\ & \boldsymbol{u} = \boldsymbol{L}\hat{\boldsymbol{K}}^{-1}\boldsymbol{G}\boldsymbol{f} \\ & \boldsymbol{f} = \boldsymbol{A}\boldsymbol{f}^{i} \\ & \boldsymbol{f}^{i} = \overline{\boldsymbol{f}^{i}} + \Delta\boldsymbol{f}^{i} \\ & \left(\Delta\boldsymbol{f}\right)^{T}\Delta\boldsymbol{f} \le 1 \end{aligned} \tag{4-20}$$

The strain energy U_A can be expressed as a function of displacement $\boldsymbol{u}$, following relation given in Eq.(4-3)

$$U_A = \boldsymbol{u}^T\boldsymbol{K}_A\boldsymbol{u} = \boldsymbol{f}^{iT}\boldsymbol{A}\boldsymbol{G}^T\hat{\boldsymbol{K}}^{-T}\boldsymbol{L}^T\boldsymbol{K}_A\boldsymbol{L}\hat{\boldsymbol{K}}^{-1}\boldsymbol{G}\boldsymbol{A}\boldsymbol{f}^{i}$$

The worst structure response can be found trough solving the problem defined in Eq.(4-21)

$$\begin{aligned} \max \quad & \left(\overline{\boldsymbol{f}^{i}} + \Delta\boldsymbol{f}^{i}\right)^{T}\boldsymbol{Q}\left(\overline{\boldsymbol{f}^{i}} + \Delta\boldsymbol{f}^{i}\right) \\ \text{s.t.} \quad & \left(\Delta\boldsymbol{f}^{i}\right)^{T}\Delta\boldsymbol{f}^{i} \le 1 \end{aligned} \tag{4-21}$$

where $\boldsymbol{Q}_A = \boldsymbol{A}\boldsymbol{G}^T\hat{\boldsymbol{K}}^{-T}\boldsymbol{L}^T\boldsymbol{K}_A\boldsymbol{L}\hat{\boldsymbol{K}}^{-1}\boldsymbol{G}\boldsymbol{A}$. This problem can be solved by using the convex modeling based method proposed in section 3.3.1. The worst load $\boldsymbol{f}^{*} = \boldsymbol{A}\left(\overline{\boldsymbol{f}^{i}} + \Delta\boldsymbol{f}^{i*}\right)$ is also

recovered during the convex model solution procedure and $U_T = \boldsymbol{f}^{*T}\boldsymbol{K}^{-1}\boldsymbol{f}^{*}$ can be evaluated accordingly.

4.2.1 Sensitivity Analysis

The solution strategy to the design problem in Eq.(4-20) follows the convex modeling based method proposed in Chapter 3. Now the sensitivity of the objective function needs to be analyzed. Differentiating the objective function $(U_A)_{\max}\left[U_T\left(\boldsymbol{f}^{*}\right)\right]$ with respect to the design variable element pseudo density a_k yields

$$\frac{d(U_A)_{\max}\left[U_T\left(\boldsymbol{f}^{*}\right)\right]}{da_k} = \frac{d(U_A)_{\max}}{da_k}\left[U_T\left(\boldsymbol{f}^{*}\right)\right] + (U_A)_{\max}\frac{d\left[U_T\left(\boldsymbol{f}^{*}\right)\right]}{da_k} \tag{4-22}$$

The calculation for the term $d(U_A)_{\max}/da_k$ follows the derivation in section 3.3.1 and can be expressed as a function of $d\boldsymbol{Q}_A/da_k$ and $d\Delta\boldsymbol{f}^{i}/da_k$, the latter one is also a function of $d\boldsymbol{Q}_A/da_k$.

For the term $d\left[U_T\left(\boldsymbol{f}^{*}\right)\right]/da_k$, it can be expanded as

$$\begin{aligned}\frac{d\left[U_T\left(\boldsymbol{f}^{*}\right)\right]}{da_k} &= \frac{d\left(\overline{\boldsymbol{f}^{i}}+\Delta\boldsymbol{f}^{i*}\right)^{T}\boldsymbol{A}^{T}\boldsymbol{K}^{-1}\boldsymbol{A}\left(\overline{\boldsymbol{f}^{i}}+\Delta\boldsymbol{f}^{i*}\right)}{da_k} \\ &= -\left(\overline{\boldsymbol{f}^{i}}+\Delta\boldsymbol{f}^{i*}\right)^{T}\boldsymbol{A}^{T}\boldsymbol{K}^{-T}\frac{\boldsymbol{K}}{da_k}\boldsymbol{K}^{-1}\boldsymbol{A}\left(\overline{\boldsymbol{f}^{i}}+\Delta\boldsymbol{f}^{i*}\right) \\ &\quad +2\left(\overline{\boldsymbol{f}^{i}}+\Delta\boldsymbol{f}^{i*}\right)^{T}\boldsymbol{A}^{T}\boldsymbol{K}^{-1}\boldsymbol{A}\left(\overline{\boldsymbol{f}^{i}}+\frac{\Delta\boldsymbol{f}^{i*}}{da_k}\right)\end{aligned} \tag{4-23}$$

The term $d\boldsymbol{K}/da_k$ is readily known and as mentioned before the $d\Delta\boldsymbol{f}^{i}/da_k$ is a function of $d\boldsymbol{Q}_A/da_k$.

As seen in Eq.(4-22) and Eq.(4-23) the sensitivity of the objective function $(U_A)_{\max}\left[U_T\left(\boldsymbol{f}^*\right)\right]$ can be expressed in terms of $d\boldsymbol{Q}_A/da_k$. Since $\boldsymbol{Q}_A = \boldsymbol{A}\boldsymbol{G}^T\hat{\boldsymbol{K}}^{-T}\boldsymbol{L}^T\boldsymbol{K}_A\boldsymbol{L}\hat{\boldsymbol{K}}^{-1}\boldsymbol{G}\boldsymbol{A}$, $d\boldsymbol{Q}_A/da_k$ can be calculated as follow:

$$\begin{aligned}\frac{d\boldsymbol{Q}_A}{da_k} &= \boldsymbol{A}^T\frac{d\boldsymbol{G}^T}{da_k}\hat{\boldsymbol{K}}^{-T}\boldsymbol{L}^T\boldsymbol{K}_A\boldsymbol{L}\hat{\boldsymbol{K}}^{-1}\boldsymbol{G}\boldsymbol{A}\\ &+\boldsymbol{A}^T\boldsymbol{G}^T\frac{d\hat{\boldsymbol{K}}^{-T}}{da_k}\boldsymbol{L}^T\boldsymbol{K}_A\boldsymbol{L}\hat{\boldsymbol{K}}^{-1}\boldsymbol{G}\boldsymbol{A}\\ &+\boldsymbol{A}^T\boldsymbol{G}^T\hat{\boldsymbol{K}}^{-T}\boldsymbol{L}^T\frac{d\boldsymbol{K}_A}{da_k}\boldsymbol{L}\hat{\boldsymbol{K}}^{-1}\boldsymbol{G}\boldsymbol{A}\\ &+\boldsymbol{A}^T\boldsymbol{G}^T\hat{\boldsymbol{K}}^{-T}\boldsymbol{L}^T\boldsymbol{K}_A\boldsymbol{L}\frac{d\hat{\boldsymbol{K}}^{-1}}{da_k}\boldsymbol{G}\boldsymbol{A}\\ &+\boldsymbol{A}^T\boldsymbol{G}^T\hat{\boldsymbol{K}}^{-T}\boldsymbol{L}^T\boldsymbol{K}_A\boldsymbol{L}\hat{\boldsymbol{K}}^{-1}\frac{d\boldsymbol{G}}{da_k}\boldsymbol{A}\end{aligned} \tag{4-24}$$

It can be identified from Eq.(4-24) that the terms $d\boldsymbol{K}_A/da_k$, $d\boldsymbol{G}/da_k$ and $d\hat{\boldsymbol{K}}^{-T}/da_k$ require evaluation. The calculation for $d\boldsymbol{K}_A/da_k$ is similar to that of $d\boldsymbol{K}/da_k$ and is not repeated. The term $d\boldsymbol{G}/da_k$ can be calculated as

$$\frac{d\boldsymbol{G}}{da_k} = \begin{bmatrix}\dfrac{d\boldsymbol{I}}{da_k}\\ \dfrac{d\boldsymbol{R}^T}{da_k}\end{bmatrix} = \begin{bmatrix}\boldsymbol{0}\\ \dfrac{d\boldsymbol{R}^T}{da_k}\end{bmatrix} \tag{4-25}$$

For the term $d\hat{\boldsymbol{K}}^{-T}/da_k$, by definition

$$\hat{\boldsymbol{K}} = \begin{bmatrix}\boldsymbol{K} & \boldsymbol{M}\boldsymbol{R}\\ \boldsymbol{R}^T\boldsymbol{M} & \boldsymbol{R}^T\boldsymbol{M}\boldsymbol{R}\end{bmatrix}$$

therefore

$$\frac{d\left(\hat{\boldsymbol{K}}^{-1}\right)}{da_k} = -\hat{\boldsymbol{K}}^{-1}\frac{d\hat{\boldsymbol{K}}}{da_k}\hat{\boldsymbol{K}}^{-1}$$

$$\frac{d\hat{\boldsymbol{K}}}{da_k} = \begin{bmatrix}\dfrac{d\boldsymbol{K}}{da_k} & \dfrac{d\boldsymbol{M}}{da_k}\boldsymbol{R}+\boldsymbol{M}\dfrac{d\boldsymbol{R}}{da_k}\\ \dfrac{d\boldsymbol{R}^T}{da_k}\boldsymbol{M}+\boldsymbol{R}^T\dfrac{d\boldsymbol{M}}{da_k} & \dfrac{d\boldsymbol{R}^T}{da_k}\boldsymbol{M}\boldsymbol{R}+\boldsymbol{R}^T\dfrac{d\boldsymbol{M}}{da_k}\boldsymbol{R}+\boldsymbol{R}^T\boldsymbol{M}\dfrac{d\boldsymbol{R}}{da_k}\end{bmatrix} \tag{4-26}$$

The terms $d\boldsymbol{R}/da_k$, $d\boldsymbol{K}/da_k$ and $d\boldsymbol{M}/da_k$ requires evaluation. The derivations for the latter two are readily known. For $d\boldsymbol{R}/da_k$, since $\boldsymbol{R}$ is defined as

$$\boldsymbol{R}=\begin{bmatrix}\begin{bmatrix}\boldsymbol{R}^1\end{bmatrix}\\ \begin{bmatrix}\boldsymbol{R}^2\end{bmatrix}\\ \vdots\\ \begin{bmatrix}\boldsymbol{R}^n\end{bmatrix}\end{bmatrix},\ \boldsymbol{R}^j=\begin{bmatrix}1 & 0 & -\left(y_j-y_{CG}\right)\\ 0 & 1 & \left(x_j-x_{CG}\right)\end{bmatrix},\ \begin{bmatrix}x_{CG}\\ y_{CG}\end{bmatrix}=\frac{1}{\sum_{i=1}^{n}m_i}\sum_{i=1}^{n}\left(m_i\begin{bmatrix}x_i\\ y_i\end{bmatrix}\right)$$

therefore

$$\frac{d\boldsymbol{R}}{da_k}=\begin{bmatrix}\begin{bmatrix}\frac{d\boldsymbol{R}^1}{da_k}\end{bmatrix}\\ \begin{bmatrix}\frac{d\boldsymbol{R}^2}{da_k}\end{bmatrix}\\ \vdots\\ \begin{bmatrix}\frac{d\boldsymbol{R}^n}{da_k}\end{bmatrix}\end{bmatrix},\ \frac{d\boldsymbol{R}^j}{da_k}=\begin{bmatrix}0 & 0 & \frac{dy_{CG}}{da_k}\\ 0 & 0 & -\frac{dx_{CG}}{da_k}\end{bmatrix} \tag{4-27}$$

where the terms dy_{CG}/da_k and dx_{CG}/da_k can be evaluated as

$$\begin{bmatrix}\frac{dx_{CG}}{da_k}\\ \frac{dy_{CG}}{da_k}\end{bmatrix}=-\left(\frac{1}{\sum_{i=1}^{n}m_i}\right)^2\frac{d\sum_{i=1}^{n}m_i}{da_k}\sum_{i=1}^{n}\left(m_i\begin{bmatrix}x_i\\ y_i\end{bmatrix}\right)+\frac{1}{\sum_{i=1}^{n}m_i}\sum_{i=1}^{n}\left(\frac{dm_i}{da_k}\begin{bmatrix}x_i\\ y_i\end{bmatrix}\right) \tag{4-28}$$

Inserting Eq. (4-28) into Eq. (4-27) gives $d\boldsymbol{R}/da_k$.

With the terms $d\boldsymbol{R}/da_k$, $d\boldsymbol{K}/da_k$ and $d\boldsymbol{M}/da_k$ evaluated, $d\boldsymbol{Q}_A/da_k$ and $d\Delta\boldsymbol{f}^i/da_k$ can be calculated. The sensitivity analysis is completed by plugging the results back to Eq.(4-22).

4.2.2 Utilizing Strain Based Topology Optimization Method

As introduced in section 3.1.1, the strain based topology optimization method proposed by Lee [36] can avoid strain distortion and stress concentration found in strain

energy based formulation. This new topology optimization method can also be employed into the protective structure design problem.

By using the strain based formulation as shown in Eq.(3-11), the protective structure design problem can be expressed as

$$\begin{aligned} \min_{\boldsymbol{a}} \quad & \left(\sum_A \bar{\varepsilon}_i^2\right)_{\max} \left[\sum_T \bar{\varepsilon}(\boldsymbol{f})_i^2\right] \\ \text{s.t.} \quad & V \le V_0 \\ & \boldsymbol{u} = \boldsymbol{L}\hat{\boldsymbol{K}}^{-1}\boldsymbol{G}\boldsymbol{f} \\ & \boldsymbol{f} = \boldsymbol{A}\boldsymbol{f}^i \\ & \boldsymbol{f}^i = \overline{\boldsymbol{f}^i} + \Delta\boldsymbol{f}^i \\ & (\Delta\boldsymbol{f})^T \Delta\boldsymbol{f} \le 1 \end{aligned} \tag{4-29}$$

where $\sum_A \bar{\varepsilon}_i^2 = \boldsymbol{u}^T \boldsymbol{K}_A^0 \boldsymbol{u}$ and $\sum_T \bar{\varepsilon}_i^2 = \boldsymbol{u}^T \boldsymbol{K}^0 \boldsymbol{u}$, the definitions for $\boldsymbol{K}_A^0$ and $\boldsymbol{K}^0$ follow the descriptions in section 3.1.1. The worst case effective strain can be evaluated by solving the problem defined in Eq.(4-30)

$$\begin{aligned} \max \quad & \left(\overline{\boldsymbol{f}^i} + \Delta\boldsymbol{f}^i\right)^T \boldsymbol{Q}\left(\overline{\boldsymbol{f}^i} + \Delta\boldsymbol{f}^i\right) \\ \text{s.t.} \quad & \left(\Delta\boldsymbol{f}^i\right)^T \Delta\boldsymbol{f}^i \le 1 \end{aligned} \tag{4-30}$$

where $\boldsymbol{Q}_A = \boldsymbol{A}\boldsymbol{G}^T \hat{\boldsymbol{K}}^{-T} \boldsymbol{L}^T \boldsymbol{K}_A^0 \boldsymbol{L}\hat{\boldsymbol{K}}^{-1}\boldsymbol{G}\boldsymbol{A}$.

The sensitivity calculation for the strain based problem in Eq.(4-29) is very similar to that of the strain energy based problem in Eq.(4-20). The only difference is when calculating the term $d\boldsymbol{Q}_A/da_k$, $d\boldsymbol{K}_A^0/da_k$ is evaluated instead of $d\boldsymbol{K}_A/da_k$ in the strain energy based problem.

With the sensitivity information ready the design problem can be solved.

4.3 Results and Discussions

In this section, the protective structure design problem introduced in Chapter 4.1 is analyzed and solved using the proposed convex modeling based method. Two examples are analyzed in this section. In the first example there is one load with uncertainty applied at the lower right corner of the unconstrained structure. In the second example four loads with uncertainties are applied simultaneously at the four corners of the structure.

4.3.1 Example 1

Considered the structure shown in Figure 4-5, the outer cushion *B* must provide protection to the content *A* under external impact. The strain based topology optimization formulation is used and the protection is measured in terms of total effective strain. Therefore the design requires minimizing the total effective strain in region *A*. The structure is unconstrained and a force with uncertainty is applied at the lower right corner.

In practice the cushion is usually made of material much lighter and softer than the content to reduce the total weight of the packaging and to absorb the majority part of the energy during impact. In this example the cushioning material in region *B* is assumed to be 1000 times lighter and 10 times softer than the content material in region *A*, or $\rho_A = 1000\rho_B$, $E_A = 10E_B$.

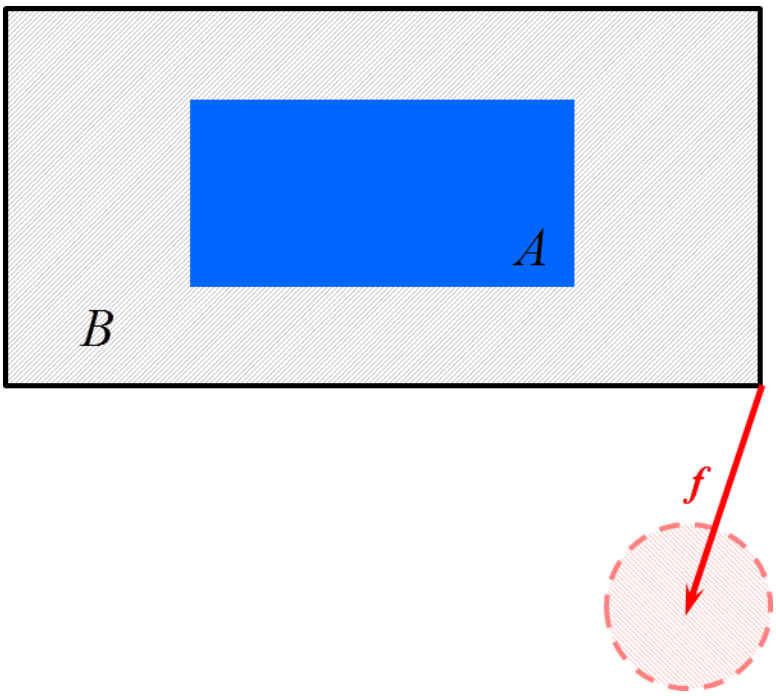

Figure 4-5 Protective Structure Design Example 1

The optimum configuration to the Figure 4-5 problem is plotted in Figure 4-6

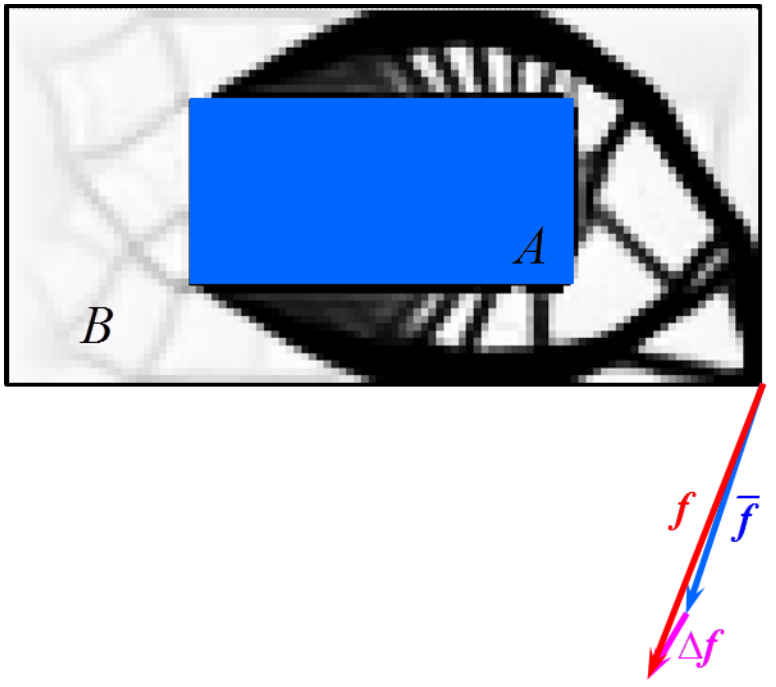

Figure 4-6 Result of the Protective Structure Design Example 1

It can be seen in the result that the content region *A* is enclosed by the shell shape protecting structures formed in region *B*. The protecting effect of the design can be proven by the percentage of total effective strain in different region under the worst case scenario. Among the total amount of effective strain, region *B* accounts for 99.98% and only 0.02% goes to region *A*, as shown in Table 4-1. Since the region *A* is subject to minimum deformation, it is well protected.

Table 4-1 Total Effective Strain under the Worst Load

	Region *A*	Region *B*	Total
Total Effective Strain	0.2	1221.6	1221.8
Percentage	0.02%	99.98%	100%

In terms of energy it can be found that the content is subject to only 0.50% of the impact energy. The cushioning absorbs almost all of the impact energy, as listed in Table 4-2. The results agree with the effective strain results and region *A* can be considered as safe.

Table 4-2 Strain Energy under the Worst Load

	Region *A*	Region *B*	Total
Strain Energy	1.9	375.2	377.1
Percentage	0.50%	99.50%	100%

4.3.2 Example 2

In this second example four loads with uncertainties are applies to the same structure described in Example 1, as seen in Figure 4-7.

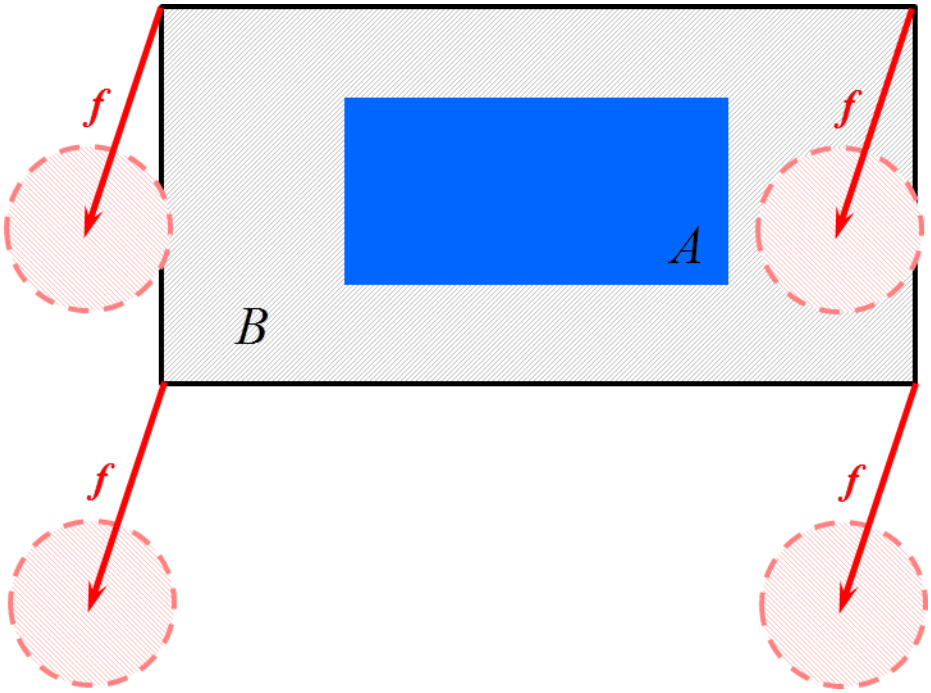

Figure 4-7 Protective Structure Design Example 2

In this example the material properties are the same as Example 1, the cushioning material is assumed to be 1000 times lighter and 10 times softer than the content material, or $\rho_A = 1000\rho_B$, $E_A = 10E_B$.

The design problem is solved by the proposed convex modeling based method and the optimized configuration is plotted in Figure 4-8. It is observed in the plot that the content is suspended by the protecting structure.

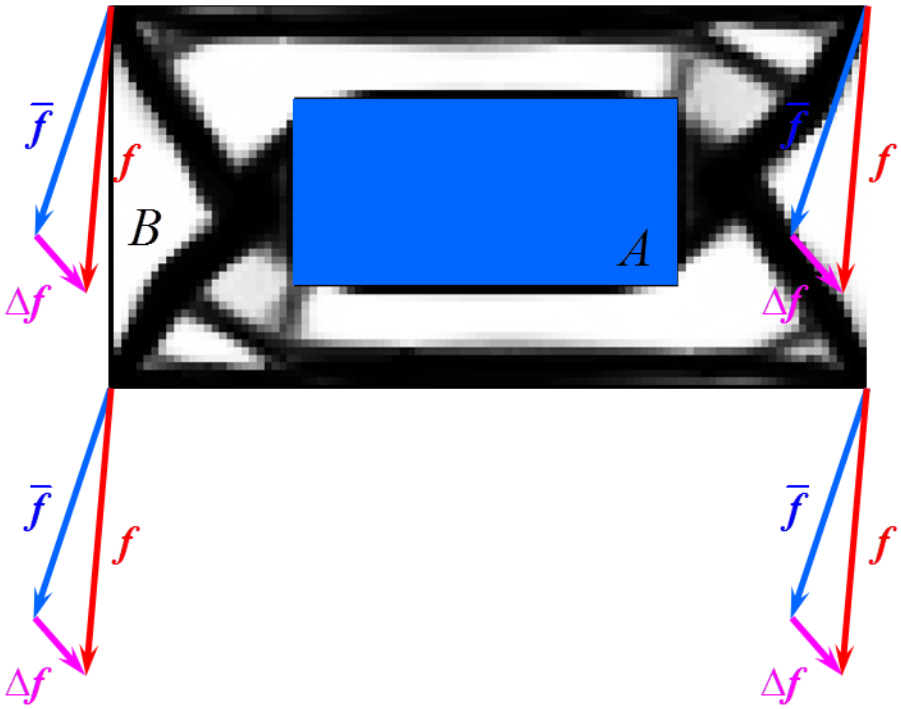

Figure 4-8 Result of the Protective Structure Design Example 2

The total effective strain of different regions is listed in Table 4-3. In this example less than 1% of total effective strain is contributed by region *A* and the majority of deformation happens in region *B*.

Table 4-3 Total Effective Strain under the Worst Load

	Region *A*	Region *B*	Total
Total Effective Strain	6.0	5642.4	5648.4
Percentage	0.11%	99.89%	100%

When analyzing the performance of the structure using strain energy it is observed that the protective structure absorbed 96.43% of the total strain energy. The content only contributes 3.57%, as shown in Table 4-4. Since under the worst case minimum amount

of strain energy was absorbed by the content, the protective structure can be considered as effective.

Table 4-4 Strain Energy under the Worst Load

	Region *A*	Region *B*	Total
Strain Energy	60.2	1624.0	1684.2
Percentage	3.57%	96.43%	100%

It is clearly demonstrated through the two protective structure design example that the convex modeling based method can evaluate the performance of the structure under the external load uncertainties. This method can be integrated with other analyzing tools and can be used to solve complicated design problems.

Chapter 5
Conclusion and Future Work

5.1 Conclusion

In this dissertation a new method, namely the convex modeling based topology optimization method, for handling external load uncertainty in structure design problem is proposed. This new method formulated the uncertainties using the non-probabilistic based model and served as a complement to the sophisticated probabilistic based method. This new method is especially useful when the distribution information of the load uncertainties is unavailable and it can be easily implemented into other analysis tools.

Developed from the truss design optimization problem, the ESCM method formulates the external load uncertainties using a convex modeling based unknown-but-bounded uncertainty formulation. The design problem is then defined following the concept of worst case design optimization: if the design satisfies the requirement under the worst condition, it can be considered safe. Therefore the design problem can be formulated as a two-level optimization problem: the lower level problem locates the worst case scenario while the upper level problem designs the optimum structure. The single-constrained lower level problem can be solved using an eigenvalue approach. The solution to the multiple-constrained lower level problem is estimated by a superposition

of the eigenvalue solutions. The sensitivity of solution to the lower level problem is then analyzed and with the sensitivity information the design problem can be solved.

The ESCM method is further integrated into the topology optimization problem, yielding the Convex Modeling Based Topology Optimization Method. This formulation extends the capability of the topology optimization method to take the external load uncertainties into consideration. The effectiveness of this convex modeling based topology optimization method is demonstrated through comparisons with conventional topology optimization formulations.

The convex modeling based topology optimization method can be implemented into other analyzing tools due to its simplicity. In this dissertation a protective structure design problem is considered. In addition to external load uncertainties, this design problem has multiple objectives and the structure itself is unconstrained. The problem is solved using the proposed convex modeling based method in conjunction with strain based topology optimization method, regional strain energy formulation and inertial relief method. The resulted structure is considered as very effective since nearly all the impact energy is absorbed by the protecting structure, leaving the content intact.

5.2 Future Work

The repeating eigenvalue situation would require further investigation. The computational efficiency can be further improved. Measures such as GPU computing can be implemented.

References

1. Vitruvius, P., et al., *De architectura*1521, Como,: Impressa p G. de Pōte, a la spese e instantia del magnifico d. A. Gallo e del nobile d. A. da Birouano. clxxxiii l.
2. Lee, K.H., et al., *Robust design for unconstrained optimization problems using the Taguchi method.* Aiaa Journal, 1996. **34**(5): p. 1059-1063.
3. Lee, K.H. and G.J. Park, *Robust optimization in discrete design space for constrained problems.* Aiaa Journal, 2002. **40**(4): p. 774-780.
4. Ditlevsen, O. and H.O. Madsen, *Structural reliability methods*1996, Chichester ; New York: Wiley. xi, 372 p.
5. Elishakoff, I., *Essay on Uncertainties in Elastic and Viscoelastic Structures - from Freudenthal,A.M. Criticisms to Modern Convex Modeling.* Computers & Structures, 1995. **56**(6): p. 871-895.
6. Ben-Haim, Y. and I. Elishakoff, *Convex models of uncertainty in applied mechanics*. Studies in applied mechanics1990, Amsterdam ; New York: Elsevier. xvii, 221 p.
7. Elishakoff, I., R.T. Haftka, and J. Fang, *Structural Design under Bounded Uncertainty - Optimization with Anti-Optimization.* Computers & Structures, 1994. **53**(6): p. 1401-1405.
8. Elishakoff, I., *Safety factors and reliability : friends or foes?*2004, Boston: Kluwer Academic Publishers.
9. Pantelides, C.P. and S. Ganzerli, *Design of trusses under uncertain loads using convex models.* Journal of Structural Engineering-Asce, 1998. **124**(3): p. 318-329.
10. Xike Zhao, H.-C.G., Limei Xu, *Non-Probabilistic Based Structural Design Optimization Under External Load Uncertainty With Eigenvalue-Superpostion of Convex Models*, in *2012 ASME International Design Engineering Technical Conferences & The Computer and Information in Engineering Conference (IDETC/CIE2012)*2012: Chicago, IL, USA.
11. Hibbeler, R.C., *Engineering mechanics : statics*. 12th ed2010, Upper Saddle River, NJ: Prentice Hall. xv, 655 p.
12. Kirsch, U., *Optimal Topologies of Truss Structures.* Computer Methods in Applied Mechanics and Engineering, 1989. **72**(1): p. 15-28.
13. Balling, R.J., R.R. Briggs, and K. Gillman, *Multiple optimum size/shape/topology designs for skeletal structures using a genetic algorithm.* Journal of Structural Engineering-Asce, 2006. **132**(7): p. 1158-1165.
14. Smith, J., et al., *Creating models of truss structures with optimization.* Acm Transactions on Graphics, 2002. **21**(3): p. 295-301.
15. Wu, P.Y., *Products of Positive Semidefinite Matrices.* Linear Algebra and Its Applications, 1988. **111**: p. 53-61.

16. Ye, Y.Y., *On Affine Scaling Algorithms for Nonconvex Quadratic-Programming.* Mathematical Programming, 1992. **56**(3): p. 285-300.
17. Jeyakumar, V., A.M. Rubinov, and Z.Y. Wu, *Non-convex quadratic minimization problems with quadratic constraints: global optimality conditions.* Mathematical Programming, 2007. **110**(3): p. 521-541.
18. Alkhayyal, F.A., C. Larsen, and T. Vanvoorhis, *A Relaxation Method for Nonconvex Quadratically Constrained Quadratic Programs.* Journal of Global Optimization, 1995. **6**(3): p. 215-230.
19. Alefeld, G. and G. Mayer, *Interval analysis: theory and applications.* Journal of Computational and Applied Mathematics, 2000. **121**(1-2): p. 421-464.
20. Qiu, Z.P. and I. Elishakoff, *Antioptimization of structures with large uncertain-but-non-random parameters via interval analysis.* Computer Methods in Applied Mechanics and Engineering, 1998. **152**(3-4): p. 361-372.
21. Helmberg, C., *Semidefinite programming.* European Journal of Operational Research, 2002. **137**(3): p. 461-482.
22. El Ghaoui, L., F. Oustry, and H. Lebret, *Robust solutions to uncertain semidefinite programs.* Siam Journal on Optimization, 1998. **9**(1): p. 33-52.
23. Kanno, Y. and I. Takewaki, *Confidence ellipsoids for static response of trusses with load and structural uncertainties.* Computer Methods in Applied Mechanics and Engineering, 2006. **196**(1-3): p. 393-403.
24. Guo, X., W. Bai, and W.S. Zhang, *Confidence extremal structural response analysis of truss structures under static load uncertainty via SDP relaxation.* Computers & Structures, 2009. **87**(3-4): p. 246-253.
25. Vandenberghe, L. and S. Boyd, *Semidefinite programming.* Siam Review, 1996. **38**(1): p. 49-95.
26. Klerk, E.d., *Aspects of semidefinite programming : interior point algorithms and selected applications*. Applied optimization2002, Dordrecht ; Boston: Kluwer Academic Publishers. xvi, 283 p.
27. Arora, J.S., *Introduction to optimum design*. 2nd ed2004, Amsterdam ; Boston: Elsevier/Academic Press. xxi, 728 p.
28. Nelson, R.B., *Simplified Calculation of Eifenvector Derivatives.* Aiaa Journal, 1976. **14**(9): p. 1201-1205.
29. Ojalvo, I.U., *Efficient Computation of Modal Sensitivities for Systems with Repeated Frequencies.* Aiaa Journal, 1988. **26**(3): p. 361-366.
30. Dailey, R.L., *Eigenvector Derivatives with Repeated Eigenvalues.* Aiaa Journal, 1989. **27**(4): p. 486-491.
31. Löfberg, J. *YALMIP : A Toolbox for Modeling and Optimization in MATLAB*. in *CACSD Conference*. 2004. Taipei, Taiwan.
32. Boyd, S.P. and L. Vandenberghe, *Convex optimization*2004, Cambridge, UK ; New York: Cambridge University Press. xiii, 716 p.
33. Bendsoe, M.P. and N. Kikuchi, *Generating Optimal Topologies in Structural Design Using a Homogenization Method.* Computer Methods in Applied Mechanics and Engineering, 1988. **71**(2): p. 197-224.
34. Bendsøe, M.P., *Optimal shape design as a material distribution problem.* Structural optimization, 1989. **1**(4): p. 193-202.

35. Bendsøe, M.P. and O. Sigmund, *Topology optimization : theory, methods, and applications*2003, Berlin ; New York: Springer. xiv, 370 p.
36. Lee, E. and Rutgers University. Graduate School--New Brunswick., *A strain based topology optimization method*, 2011. p. x, 112 p.
37. Kharmanda, G., et al., *Reliability-based topology optimization.* Structural and Multidisciplinary Optimization, 2004. **26**(5): p. 295-307.
38. Jung, H.S. and S. Cho, *Reliability-based topology optimization of geometrically nonlinear structures with loading and material uncertainties.* Finite Elements in Analysis and Design, 2004. **41**(3): p. 311-331.
39. Ayyub, B.M., *Uncertainty modeling and analysis in civil engineering*1998, Boca Raton: CRC Press. 506 p.
40. Wang, N. and Y. Yang, *Optimization of Structures under Load Uncertainties Based on Hybrid Genetic Algorithm*. Evolutionary Computation2009.
41. Elishakoff, I. and M. Ohsaki, *Optimization and anti-optimization of structures under uncertainty*2010, London Hackensack, NJ: Imperial College Press ; Distributed by World Scientific. xxii, 402 p.
42. Gerhard, V. and H. Raphael, *A two species genetic algorithm for designing composite laminates subjected to uncertainty*, in *37th Structure, Structural Dynamics and Materials Conference*1996, American Institute of Aeronautics and Astronautics.
43. Mattheij, R.M.M. and G. Soderlind, *On Inhomogeneous Eigenvalue Problems .1*. Linear Algebra and Its Applications, 1987. **88-9**: p. 507-531.
44. Grzegorski, S., *On the Solutions of Inhomogeneous Symmetric Eigenvalue Problem.* Actual Problems of Economics, 2010(108): p. 297-300.
45. Gea, H.C., *Applications of regional strain energy in compliant structure design for energy absorption.* Structural and Multidisciplinary Optimization, 2004. **26**(3-4): p. 224-228.
46. Min, S., et al., *Optimal topology design of structures under dynamic loads.* Structural Optimization, 1999. **17**(2-3): p. 208-218.
47. Lee, Y.-L., M.E. Barkey, and H.-T. Kang, *Metal fatigue analysis handbook : practical problem-solving techniques for computer-aided engineering*2012, Waltham, MA: Butterworth-Heinemann. l, 580 p.
48. Anvari, M. and B. Beigi, *Automotive Body Fatigue Analysis–Inertia Relief or Transient Dynamics?* SAE Technical Paper, 1999: p. 01-3149.
49. Wei Song, H.C.G., Re-Jye Yang, Ching-Hung Chuang. *Application of Regional Strain Energy in Topology Optimization with Inertia Relief Analysis*. in *ASME 2013 International Design Engineering Technical Conferences & Computers and Information in Engineering Conference (IDETC/CIE 2013)*. 2013. Portland, OR, USA.
50. Hibbeler, R.C., *Mechanics for engineers. Dynamics*1985, New York London: Macmillan; Collier Macmillan. xii, 393 p.

Curriculum VITA

Xike Zhao

2004-2008	Bachelor of Science Mechanical Engineering Tongji University, Shanghai, China
2008-2013	PhD Candidate Mechanical Engineering Rutgers University, New Brunswick, NJ, USA
2012-2013	Mechanical Engineering Intern WM Steinen Manufacturing Co., Ltd, Parsippany, NJ, USA
2013-	Mechanical Design Engineer Heller Industries, Florham Park, NJ, USA
Publications	"Non-Probabilistic Based Structural Design Optimization under External Load Uncertainty with Eigenvalue-Superposition of Convex Models", 2012 ASME (IDETC/CIE2012) "Application of Eigenvalue-Superposition of Convex Models Method in Topology Optimization under Load Uncertainties", 2013 ASME (IDETC/CIE2013)